# Appendix A
# Computing Lyapunov Exponents for Time-Delay Systems

## A.1 Introduction

The hall mark property of a chaotic attractor, namely sensitive dependence on initial condition, has been associated by the Lyapunov exponents to characterize the degree of exponential divergence/convergence of trajectories arising from nearby initial conditions. At first, we will describe briefly the concept of Lyapunov exponent and the procedure for computing Lyapunov exponents of the flow of a dynamical system described by n-dimensional ordinary differential equations (ODEs), which is then extended to scalar delay differential equations (DDEs), which are essentially an infinite-dimensional systems. An important step in computing Lyapunov exponents of DDEs is that it is necessary to approximate the continuous evolution of an infinite-dimensional system by a finite-dimensional (appreciably large) iterated mapping. Then the Lyapunov exponents of the finite-dimensional map can be calculated by computing simultaneously the reference trajectories from the original map and the trajectories from their linearized equations of motion. Alternatively, it can also be calculated by computing the evolution of infinitesimal volume element formed by a set of infinitesimal separation vectors corresponding to the trajectories starting from nearby initial conditions.

## A.2 Lyapunov Exponents of an n-Dimensional Dynamical System

Consider an n-dimensional dynamical system described by the system of first order coupled ordinary differential equation [1–3]

$$\dot{\mathbf{X}} = \mathbf{F}(\mathbf{X}), \tag{A.1}$$

where $\mathbf{X}(t) = (x_1(t), x_2(t), ..., x_n(t))$. We consider two trajectories in the $n$-dimensional phase space starting from two nearby initial conditions $\mathbf{X}_0$ and $\mathbf{X}'_0 = \mathbf{X}_0 + \delta\mathbf{X}_0$. They evolve with time yielding the vectors $\mathbf{X}(t)$ and $\mathbf{X}'(t) = \mathbf{X}(t) + \delta\mathbf{X}(t)$, respectively, with the Euclidean norm

M. Lakshmanan, D.V. Senthilkumar, *Dynamics of Nonlinear Time-Delay Systems*,
Springer Series in Synergetics, DOI 10.1007/978-3-642-14938-2,

$$d\left(\mathbf{X}_0, t\right) = ||\delta\mathbf{X}\left(\mathbf{X}_0, t\right)|| \equiv \sqrt{\delta x_1^2 + \delta x_2^2 + ... + \delta x_n^2}\ . \tag{A.2}$$

Here $d(\mathbf{X}_0, t)$ is simply a measure of the distance between the two trajectories $\mathbf{X}(t)$ and $\mathbf{X}'(t)$. The time evolution of $\delta\mathbf{X}$ is found by linearizing (A.1) to obtain

$$\delta\dot{\mathbf{X}} = M(\mathbf{X}(t))\ .\ \delta\mathbf{X}\ , \tag{A.3}$$

where $M = \partial\mathbf{F}/\partial\mathbf{X}|_{\mathbf{X}=\mathbf{X}_0}$ is the Jacobian matrix of $\mathbf{F}$. Then the mean rate of divergence of two close trajectories is given by

$$\lambda\left(\mathbf{X}_0, \delta\mathbf{X}\right) = \lim_{t\to\infty} \frac{1}{t} \log\left(\frac{d\left(\mathbf{X}_0, t\right)}{d\left(\mathbf{X}_0, 0\right)}\right)\ . \tag{A.4}$$

Furthermore, there are $n$-orthonormal vectors $\mathbf{e}_i$ of $\delta\mathbf{X}$, $i = 1, 2, ..., n$, such that

$$\delta\dot{\mathbf{e}}_i = M\left(\mathbf{X}_0\right)\mathbf{e}_i\ , \quad M = \mathrm{diag}\left(\lambda_1, \lambda_2, ..., \lambda_n\right)\ . \tag{A.5}$$

That is, there are $n$-Lyapunov exponents given by

$$\lambda_i\left(\mathbf{X}_0\right) = \lambda_i\left(\mathbf{X}_0, \mathbf{e}_i\right)\ , \quad i = 1, 2, ..., n\ . \tag{A.6}$$

These can be ordered as $\lambda_1 \geq \lambda_2 \geq ... \geq \lambda_n$. From (A.4) and (A.6) we may write

$$d_i\left(\mathbf{X}_0, t\right) \approx d_i\left(\mathbf{X}_0, 0\right) \mathrm{e}^{\lambda_i t}\ , \quad i = 1, 2, ..., n\ . \tag{A.7}$$

To identify whether the motion is periodic or chaotic it is sufficient to consider the largest nonzero Lyapunov exponent $\lambda_m$ among the $n$ Lyapunov exponents of the n-dimensional dynamical system.

### *A.2.1 Computation of Lyapunov Exponents*

To compute the $n$-Lyapunov exponents of the $n$-dimensional dynamical system (A.1), a reference trajectory is created by integrating the nonlinear equations of motion (A.1). Simultaneously the linearized equations of motion (A.3) are integrated for $n$-different initial conditions defining an arbitrarily oriented frame of $n$-orthonormal vectors ($\Delta\mathbf{X}_1$, $\Delta\mathbf{X}_2$, ..., $\Delta\mathbf{X}_n$). There are two technical problems [4] in evaluating the Lyapunov exponents directly using (A.4), namely the variational equations have at least one exponentially diverging solution for chaotic dynamical systems leading to a storage problem in the computer memory. Further, the orthonormal vectors evolve in time and tend to fall along the local direction of most rapid growth. Due to the finite precision of computer calculations the collapse toward a common direction causes the tangent space orientation of all the vectors to become indistinguishable. Both the problems can be overcome by a repeated use of what is

known as Gram-Schmidt reorthonormalization (GSR) procedure [5] which is well known in the theory of linear vector spaces. We apply GSR after $\tau$ time steps which orthonormalize the evolved vectors to give a new set $\{\mathbf{u}_1, \mathbf{u}_2, ..., \mathbf{u}_n\}$:

$$\mathbf{v}_1 = \Delta\mathbf{X}_1 \ , \tag{A.8}$$

$$\mathbf{u}_1 = \mathbf{v}_1/||\mathbf{v}_1|| \ , \tag{A.9}$$

$$\mathbf{v}_i = \Delta\mathbf{X}_i - \sum_{j=1}^{i-1} \langle \Delta\mathbf{X}_i \ , \mathbf{u}_j \rangle \ \mathbf{u}_j \ , \quad i = 2, 3, ..., n \tag{A.10}$$

$$\mathbf{u}_i = \mathbf{v}_i/||\mathbf{v}_i|| \ , \tag{A.11}$$

where $\langle , \rangle$ denotes inner product. In this way the rate of growth of evolved vectors can be updated by the repeated use of GSR. Then, after the $N$-th stage, for $N$ large enough, the one-dimensional Lyapunov exponents are given by

$$\lambda_i = \frac{1}{N\tau} \sum_{k=1}^{N} \log ||\mathbf{v}_i^{(k)}|| \ . \tag{A.12}$$

For a given dynamical system, $\tau$ and $N$ are chosen appropriately so that the convergence of Lyapunov exponents is assured. A fortran code algorithm implementing the above scheme can be found in [4].

## A.3 Lyapunov Exponents of a DDE

As described in the Sect. 1.2.2 of Chap. 1, a DDE of the form

$$\dot{X} = F(t, X(t), X(t - \tau)), \tag{A.13}$$

can be approximated as an $N$-dimensional iterated map [6], $X(k + 1) = G(X(k))$, ($k$ labels the $k$th iteration and $k + 1$ to its next iteration). Now, the Lyapunov exponents of the $N$-dimensional map can be calculated by computing simultaneously a reference trajectory and the trajectories that are separated from the reference trajectory by a small amount, corresponding to N-different initial conditions defining an arbitrarily oriented frame of N-orthonormal vectors as described above.

Alternatively, it can also be calculated by computing the evolution of infinitesimal volume element, formed by a set of infinitesimal separation vectors $\delta x$, which evolves according to

$$\delta x(k + 1) = \sum_{i=1}^{N} \frac{\partial G(x(k))}{\partial x_i(k)} \delta x_i(k). \tag{A.14}$$

Computational problems associated with computing adjacent trajectories can be avoided by calculating the evolution of infinitesimal separations directly from the above equation. The evolution equation of the infinitesimal volume element corresponding to the continuous DDE (A.13) can be written as

$$\frac{d\delta x}{dt} = \frac{\partial F(x, x_\tau)}{\partial x}\delta x + \frac{\partial F(x, x_\tau)}{\partial x_\tau}\delta x_\tau. \tag{A.15}$$

This equation can be solved using any convenient integration scheme. The small separations $\delta x$ represents separation between two infinite-dimensional vectors. There are $N$ such separations for every coordinate of the $N$-dimensional system corresponding to $N$ Lyapunov exponents. Let $\delta\tilde{x}^i(k)$ denote the collection of all separations of $i$th coordinate during $k$th iteration, then its Lyapunov exponents can be given as

$$\lambda_i = \frac{1}{L\tau}\sum_{k=1}^{L} \log \frac{||\delta\tilde{x}^i(k)||}{||\delta\tilde{x}^i(k-1)||}. \tag{A.16}$$

For computing each exponent $\lambda_i$, arbitrarily select an initial separation $\delta\tilde{x}^i(0)$ and integrate for a time $\tau$. Renormalize $\delta\tilde{x}^1(\tau)$ to have unit length. Using GSR procedure, orthonormalize the second separation function relative to the first, the third relative to the second, and so on. Repeat this procedure for $L$ iterations. For sufficiently large $L$, it is numerically shown that the values of $\lambda_i$ converge [6].

## References

1. M. Lakshmanan, S. Rajasekar, *Nonlinear Dynamics: Integrability, Chaos and Patterns* (Springer, Berlin, 2003)
2. J.P. Eckmann, D. Ruelle, Rev. Mod. Phys. **57**, 617 (1985)
3. H.G. Schüster, *Deterministic Chaos* (Physik Verlag, Weinheim, 1984)
4. A. Wolf, J.B. Swift, H.L. Swinney, J. A. Vastano, Physica D **16**, 285 (1985)
5. C.R. Wylie, L.C. Barrett, *Advanced Engineering Mathematics* (McGraw-Hill, New York, 1995)
6. J.D. Farmer, Physica D **4**, 366 (1982)

# Appendix B
# A Brief Introduction to Synchronization in Chaotic Dynamical Systems

## B.1 Introduction

Synchronization phenomenon is abundant in nature and can be realized in very many problems of science, engineering, and social life. Systems as diverse as clocks, singing crickets, cardiac pacemakers, firing neurons, and applauding audiences exhibit a tendency to operate in synchrony. The underlying phenomenon is universal and can be understood within a common framework based on modern nonlinear dynamics.

The history of synchronization goes back to the seventeenth century when the Dutch physicist Christiaan Huygens reported on his observation of phase synchronization of two pendulum clocks [1, 2]. Huygens briefly, but extremely precisely, described his observation of synchronization as follows.

> ... It is quite worth noting that when we suspended two clocks so constructed from two hooks imbedded in the same wooden beam, the motions of each pendulum in opposite swings were so much in agreement that they never receded the least bit from each other and the sound of each was always heard simultaneously. Further, if this agreement was disturbed by some interference, it reestablished itself in a short time. For a long time I was amazed at this unexpected result, but after a careful examination finally found that the cause of this is due to the motion of the beam, even though this is hardly perceptible. The cause is that the oscillations of the pendula, in proportion to their weight, communicate some motion to the clocks. This motion, impressed onto the beam, necessarily has the effect of making the pendula come to a state of exactly contrary swings if it happened that they moved otherwise at first, and from this finally the motion of the beam completely ceases. But this cause is not sufficiently powerful unless the opposite motions of the clocks are exactly equal and uniform.

Despite being the oldest scientifically studied nonlinear effects, synchronization was understood only in the 1920s when Edward Appleton [3] and Balthasar van der Pol [4] theoretically and experimentally studied synchronization of triode oscillators. Considering the simplest case, they showed that the frequency of a generator can be entrained, or synchronized, by a weak external signal of a slightly different frequency. These studies were of great practical importance because triode generators became the basic elements of radio communication systems. The

synchronization phenomenon was used to stabilize the frequency of a powerful generator with the help of one which was weak but very precise.

Even though the notion of *synchronization* was identified well before the concept of chaos was realized, it was believed that *chaotic synchronization* was not feasible because of the hallmark property of chaos which is the extreme sensitivity to initial conditions. The latter property implies that two trajectories emerging from two different close by initial conditions separate exponentially in the course of time. As a result, chaotic systems intrinsically defy synchronization because even two identical systems starting from very slightly different initial conditions would evolve in time in an unsynchronized manner (the differences in the system states would grow exponentially). This is a relevant practical problem, insofar as experimental initial conditions are never known perfectly. Nevertheless, it has been shown that it is possible to synchronize chaotic systems, to make them evolve on the same chaotic trajectory, by introducing appropriate coupling between them due to the works of Pecora and Carroll and the earlier works of Fujisaka and Yamada [5–10]. Since the identification of synchronization in chaotic oscillators, the phenomenon has attracted considerable research activity in different areas of science and technology and several generalizations and interesting applications have been developed. The phenomenon of chaotic synchronization is of interest not only from a theoretical point of view but also has potential applications in diverse subjects such as as biological, neurological, laser, chemical, electrical and fluid mechanical systems as well as in secure communication, cryptography, system reconstruction, parameter estimation, controlling chaos, long term prediction of chaotic systems and so on [2, 11–21].

*Chaotic synchronization*, in general, can be defined as a process wherein two (or many) chaotic systems (either equivalent or nonequivalent) adjust a given property of their motion to a common behavior, due to coupling or forcing. This ranges from complete agreement of trajectories to locking of phases [11].

The first point we note here is that there is a great difference in the process leading to synchronized states, depending upon the particular coupling configuration, namely one should distinguish two main cases: unidirectional coupling and bidirectional coupling. When the evolution of one of the coupled systems is unaltered by the coupling, the resulting configuration is called *unidirectional coupling* or *drive-response coupling*. As a result, the response system is slaved to follow the dynamics of the drive system, which, instead, purely acts as an external but chaotic forcing for the response system. In such a case external synchronization is produced. Typical examples are communication using chaos. On the contrary, when both the systems are connected in such a way that they mutually influence each other's behavior then the corresponding configuration is called *bidirectional coupling*. Here both the systems are coupled with each other, and the coupling factor induces an adjustment of the rhythms onto a common synchronized manifold, thus inducing a mutual synchronization behavior. This situation typically occurs in physiology, e.g. between cardiac and respiratory systems or between neurons. These two processes are very different not only from a philosophical point of view; up to now no way has been discovered to reduce one process to another, or to link formally the two cases. Inside this classification, the appearance and robustness of synchronization states have

been established by means of several different coupling schemes, such as the Pecora and Carrol method [8, 10, 21], the negative feedback [14], the sporadic driving [22], the active-passive decomposition [23, 24], the diffusive coupling and some other hybrid methods [25]. A description and analysis of some of these coupling schemes is given in [26] in a single mathematical framework. In the following studies we will consider only the so called *unidirectional coupling* or *drive-response coupling* configuration.

Chaos synchronization has been receiving a great deal of interest for more than two decades in view of its potential applications in various fields of science and engineering [5, 6, 8, 27–29]. Since the identification of chaotic synchronization, different kinds of synchronization have been proposed in interacting chaotic systems, which have all been identified both theoretically and experimentally. These include

1. complete or identical synchronization (CS) [5–8, 27],
2. phase synchronization (PS) [30–32],
3. lag synchronization (LS) [33–35],
4. anticipatory synchronization (AS) [36–38],
5. generalized synchronization (GS) [39–41],
6. intermittent lag synchronization (ILS) [33, 42–44],
7. intermittent anticipatory synchronization (IAS) [45],
8. intermittent generalized synchronization (IGS) [46],
9. imperfect or intermittent phase synchronization (IPS) [47–50],
10. almost synchronization (AS) [51],
11. time scale synchronization (TSS) [52] and
12. episodic synchronization (ES) [53].

Transition from one kind of synchronization to the other, coexistence of different kinds of synchronization in time series and also the nature of transitions have also been studied extensively [33–35, 54, 55] in coupled chaotic systems. There are also attempts to find a unifying framework for defining the overall class of chaotic synchronizations [56–58]. Before presenting the details of important types of aforesaid synchronization phenomena, we will discuss about the characterization for identifying the existence of synchronization in coupled chaotic systems.

## B.2 Characterization of Synchronization

The existence of synchronization, in particular CS, is also characterized by quantitative measures in addition to qualitative pictures such as combined phase space plots of state variables, time trajectory of error variable, etc. Such quantitative measures are usually addressed in terms of a stability problem, that is, stability of the synchronized motion, and many criteria have been established in the literature to cope with it. One of the most popular and widely used criteria is the use of the

Lyapunov exponents as average measurements of expansion or shrinkage of small displacements along the synchronized trajectory.

Let us consider a set of two unidirectionally coupled identical chaotic systems whose temporal evolution is given by the system of coupled first order ODEs

$$\dot{\mathbf{X}} = F(\mathbf{X}), \qquad \left(\dot{} = \frac{d}{dt}\right) \tag{B.1a}$$

$$\dot{\mathbf{Y}} = F(\mathbf{Y}, \mathbf{S}(t)), \tag{B.1b}$$

where $\mathbf{X} = (x_1, x_2, ..., x_n)$ and $\mathbf{Y} = (y_1, y_2, ..., y_n)$ are n-dimensional state vectors corresponding to the drive and response systems, respectively, with $F$ defining a vector field $F : R^n \rightarrow R^n$ and $\mathbf{S}(t)$ is some function of $\mathbf{X}(t)$, corresponding to the drive signal. The stability problem of identical coupled systems can be formulated in a very general way by addressing the question of the stability of the CS manifold $\mathbf{X} \equiv \mathbf{Y}$, or equivalently by studying the temporal evolution of the synchronization error $\mathbf{e} \equiv \mathbf{Y} - \mathbf{X}$. The evolution of $\mathbf{e}$ is given by

$$\dot{\mathbf{e}} = F(\mathbf{X}) - F(\mathbf{Y}, \mathbf{S}(t)). \tag{B.2}$$

A CS regime exists when the synchronization manifold is asymptotically stable for all possible trajectories $\mathbf{S}(t)$ of the driving system within the chaotic attractor. This property can be proved by carrying out a stability analysis of the linearized system for small $\mathbf{e}$,

$$\dot{\mathbf{e}} = \mathbf{D}_X(\mathbf{S}(t))\mathbf{e}, \tag{B.3}$$

where $\mathbf{D}_X$ is the Jacobian of the vector field $\mathbf{F}$ evaluated onto the driving trajectory $\mathbf{S}(t)$. Normally, when the driving trajectory $\mathbf{S}(t)$ is constant (fixed point) or periodic (limit cycle), the stability problem can be studied by evaluating the eigenvalues of $\mathbf{D}_X$ or the Floquet multipliers [59, 60]. However, if the response systems is driven by a chaotic signal, this method will not work.

A possible way out is to calculate the Lyapunov exponents of the system (B.3). In the context of drive-response coupling schemes, these exponents are usually called *conditional Lyapunov exponents* (CLEs) because they are the Lyapunov exponents of the response system under the explicit constraint that they must be calculated on the trajectory $\mathbf{S}(t)$ [10, 23]. Alternatively, they are called *transverse Lyapunov exponents* (TLEs) because they correspond to directions which are transverse to the synchronization manifold $\mathbf{X} \equiv \mathbf{Y}$ [25, 61]. These exponents may be defined, for an initial condition of the driver signal $\mathbf{S}_0$ and initial orientation of the infinitesimal displacement $\mathbf{U}_0 = \mathbf{e}(0)/|\mathbf{e}(0)|$, as

$$h(\mathbf{S}_0, \mathbf{U}_0) \equiv \lim_{t\rightarrow\infty} \frac{1}{t} ln \left(\frac{|\mathbf{e}(t)|}{|\mathbf{e}(0)|}\right) = \lim_{t\rightarrow\infty} \frac{1}{t} ln|\mathbf{Z}(\mathbf{S}_0, t).\mathbf{U}_0|, \tag{B.4}$$

where $\mathbf{Z}(\mathbf{S}_0, t)$ is the matrix solution of the linearized equation,

$$d\mathbf{Z}/dt = \mathbf{D}_X(\mathbf{S}(t))\mathbf{Z}, \tag{B.5}$$

subject to the initial condition $\mathbf{Z}(0) = I$. The synchronization error $\mathbf{e}$ evolves according to $\mathbf{e(t)} = \mathbf{Z}(\mathbf{S}_0, t)\mathbf{e_0}$ and then the matrix $\mathbf{Z}$ determines whether this error shrinks or grows in a particular direction. In most cases, however, the calculation cannot be made analytically, and therefore numerical algorithms should be used [62–64].

It is very important to emphasize that the negativity of the conditional Lyapunov exponents is only a necessary condition for the stability of the synchronized state. The conditional Lyapunov exponents are obtained from a temporal average, and therefore they characterize the global stability over the whole chaotic attractor. Relevant cases exist where these exponents are negative and nevertheless the systems are not perfectly synchronized, thus indicating that additional conditions should be fulfilled to warrant synchronization in a necessary and sufficient way [65].

The stability of a CS manifold can also be studied by the use of the Lyapunov function $L(\mathbf{e})$. It can be defined as a continuously differentiable real valued function with the following properties:

(a) $L(\mathbf{e}) > 0$ for all $\mathbf{e} \neq 0$ and $L(\mathbf{e}) = 0$ for $\mathbf{e} = 0$.
(b) $dL/dt < 0$ for all $\mathbf{e} \neq 0$.

If for a given coupled system one can find a Lyapunov function, then the CS manifold is globally stable. For illustrative examples one may refer to [13, 23, 28, 66]. Unfortunately, whether such functions exist and how one should construct them is known only in a very limited number of cases, whereas a general procedure to obtain these functions is not yet available.

At this stage, let us summarize the validity of the stability criteria discussed above. In general, only Lyapunov functions give a sufficient condition for the stability of the synchronization manifold, whereas the negativity of the conditional Lyapunov exponents provides a necessary condition. While the Lyapunov function criterion gives a local condition for stability, the other two (CLEs/TLEs) involve temporal averages over chaotic trajectories of the driving signal, and therefore they establish conditions for global stability. As a consequence, none of these latter criteria prevents from local desynchronization events that could occur within the CS manifold. This point is discussed in [61], where the synchronized behavior of two chaotic circuits coupled in a drive-response configuration is studied. The appearance of these local desynchronized states, despite Lyapunov exponents being negative, is also related with a small parameter mismatch between the coupled systems and low levels of noise, which are unavoidable effects in experimental devices and in numerical integration.

We have pointed in the above that the characterization of synchronization in coupled identical systems can be done using the stability of synchronized motion by referring to the stability of the CS manifold. When we deal with nonidentical

coupled systems, similar stability criteria can be formulated, but additional problem will appear due to the more complicated structure of the synchronization manifold. Also, the other kinds of synchronization have their own characterizations, which we will discuss in the following sections.

### *B.2.1 Complete Synchronization*

When one deals with coupled identical chaotic systems, synchronization appears as the equality of the state variables while evolving in time. Complete synchronization (CS) was the first discovered and simplest form of synchronization in chaotic systems. It is characterized by a perfect locking of the chaotic trajectories of two identical nonlinear systems which is achieved by means of a suitable coupling in such a way that the two trajectories remain in step with each other in the course of time, that is, $X(t) \equiv Y(t)$, where $X$ and $Y$ are n-dimensional state variables whose evolution is represented by (B.1), individually. This mechanism was first shown to occur when two identical chaotic systems are coupled unidirectionally, provided the conditional Lyapunov exponents of the subsystem (response) to be synchronized are all negative [8]. Complete synchronization is also called conventional synchronization or identical synchronization in the literature [67].

As an illustrative example for CS, we will consider a Pecora and Caroll drive-response configuration with a drive system given by the Lorenz system [68],

$$\dot{x}_1 = \sigma(y_1 - x_1), \tag{B.6a}$$
$$\dot{y}_1 = -x_1 z_1 + r x_1 - y_1, \tag{B.6b}$$
$$\dot{z}_1 = x_1 y_1 - b z_1, \tag{B.6c}$$

and with a response system given by the subspace containing the $(y, z)$ variables, where $x_1$ acts as the driving signal for the response system,

$$\dot{y}_2 = -x_1 z_2 + r x_1 - y_2, \tag{B.7a}$$
$$\dot{z}_2 = x_1 y_2 - b z_2. \tag{B.7b}$$

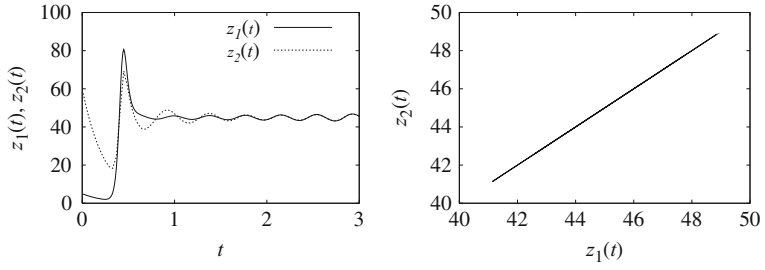


**Fig. B.1** Complete synchronization between two coupled Lorenz systems using Pecora and Caroll method as represented by Eqs. (B.6) and (B.7). (**a**) Time trajectory plot and (**b**) Phase space plot

Here the control parameters $\sigma, r$ and $b$ are fixed as $\sigma = 16, r = 45.92$ and $b = 4$ so that Eqs. (B.6) give rise to chaotic dynamics. With this particular choice of the driving, CS sets in rather quickly as shown in Fig. B.1. Figure B.1a is a time trajectory plot of $z_1(t)$ and $z_2(t)$ showing complete synchronization and diagonal line in Fig. B.1b confirms the CS between $z_1(t)$ and $z_2(t)$. Note that the above configuration is also called a *homogeneous driving* configuration.

### *B.2.2 Phase Synchronization*

Definition of chaotic phase synchronization (CPS) in coupled chaotic systems is derived from the classical definition of phase synchronization in periodic oscillators. Interacting chaotic systems are said to be in phase synchronized state when there exists entrainment between phases of the systems, $n\phi_1 - m\phi_2 =$const, while their amplitudes may remain chaotic and uncorrelated (In the presence of noise, a weaker condition for phase locking, $|n\phi_1 - m\phi_2| <$const, should be used instead). In other words, CPS exists when their respective frequencies and phases are locked [2, 11, 69]. To study CPS, one has to identify a well defined phase variable in both the coupled systems. If the flow of the chaotic oscillator has a proper rotation around a certain reference point, the phase can be defined in a straightforward way. For example, for the Rössler system [30] with standard parameters the projection of the chaotic attractor onto the $(x, y)$ plane looks like a smeared limit cycle. In this and similar cases one can define the phase [2, 11] as

$$\phi(t) = \arctan(y(t)/x(t)). \tag{B.8}$$

A more general approach to define the phase in chaotic oscillators is the analytic signal approach [2, 11] introduced in [70]. The analytic signal $\chi(t)$ is given by

$$\chi(t) = s(t) + i\tilde{s}(t) = A(t)\exp^{i\Phi(t)}, \tag{B.9}$$

where $\tilde{s}(t)$ denotes the Hilbert transform of the observed scalar time series $s(t)$

$$\tilde{s}(t) = \frac{1}{\pi} P.V. \int_{-\infty}^{\infty} \frac{s(t')}{t - t'} dt', \tag{B.10}$$

where P.V. stands for the Cauchy principle value of the integral and this method is especially useful for experimental applications [2, 11] .

The phase of a chaotic attractor can also be defined based on an appropriate Poincaré surface of section which the chaotic trajectory crosses once for each rotation. Each crossing of the orbit with the Poincaré section corresponds to an increment of $2\pi$ of the phase, and the phase in between two crossings is linearly interpolated [2, 11],

$$\Phi(t) = 2\pi k + 2\pi \frac{t - t_k}{t_{k+1} - t_k}, \qquad (t_k < t < t_{k+1}) \tag{B.11}$$

where $t_k$ is the time of $k$th crossing of the flow with the Poincaré section. For the phase coherent chaotic oscillators, that is, for flows which have a proper rotation around a certain reference point, the phases calculated by these three different ways are in good agreement [2, 11].

As the simplest example of chaotic phase synchronization, we will consider two coupled Rössler systems [30, 71],

$$\dot{x}_{1,2} = -\omega_{1,2} y_{1,2} - z_{1,2} + C(x_{2,1} - x_{1,2}), \tag{B.12a}$$
$$\dot{y}_{1,2} = \omega_{1,2} x_{1,2} + a y_{1,2}, \tag{B.12b}$$
$$\dot{z}_{1,2} = 0.2 + z_{1,2}(x_{1,2} - 10), \tag{B.12c}$$

where the parameters $\omega_{1,2} = 1 \pm \Delta\omega$ govern the frequency mismatch and $C$ is the strength of coupling. As the coupling is increased for a fixed mismatch $\Delta\omega$, one can observe a transition from a regime, where the phases rotate with different velocities $\phi_1 - \phi_2 \sim \Delta\Omega t$, to a synchronous state, where the phase difference does not grow with time $|\phi_1 - \phi_2| < \text{const}$; $\Delta\Omega = 0$. This transition is illustrated in Fig. B.2a. Moreover, the correlation between the amplitudes of $x_1$ and $x_2$ is quite small (Fig. B.2b), although the phases are completely locked. In this example, it is shown that transition of one of the zero Lyapunov exponents to negative value as shown in Fig. B.3 corresponds to the critical point at which the phases become locked. It is known that in the absence of coupling each oscillator has one positive, one negative and one zero Lyapunov exponents. The zero Lyapunov exponents correspond to the transition along the trajectory. As the coupling strength is increased the interaction between the oscillators increases such that the phase difference $\phi_1 - \phi_2$ decreases and phases become locked eventually. Thus one of the zero exponents becomes negative to account for the phase locking phenomenon.

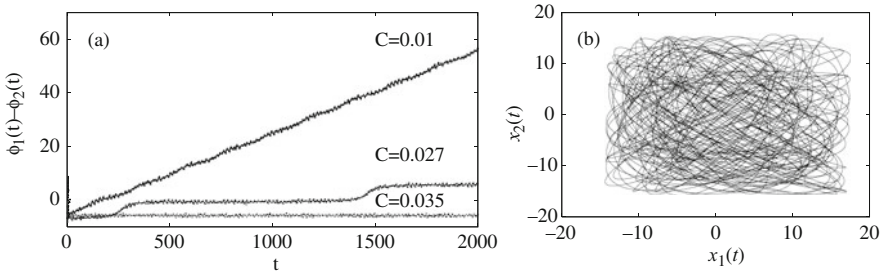


**Fig. B.2** (**a**) Phase difference of two coupled Rössler systems (B.12) versus time for nonsynchronous ($C = 0.01$), nearly synchronous ($C = 0.027$) and synchronous ($C = 0.035$) states and (**b**) Amplitudes of (B.12) that remain uncorrelated for phase synchronous case. The frequency mismatch is $\Delta\omega = 0.015$ and the value of the parameter $a = 0.15$

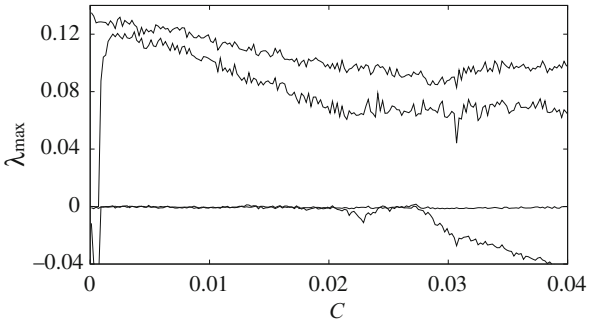


**Fig. B.3** The four largest Lyapunov exponents of coupled coupled Rössler systems (B.12) as a function of the coupling strength $C$

### *B.2.3 Lag Synchronization*

It has been shown in the previous section that when nonidentical chaotic oscillators are weakly coupled, the phases can be locked while the amplitudes remain highly uncorrelated. On further increase of the coupling strength, a relationship between the amplitudes may be established. Indeed, it has been demonstrated that there exists a regime of *lag synchronization* [33] where the states of the two oscillators are nearly identical, but one system lags in time with the other, that is, $Y(t) = X(t-\tau)$, $\tau > 0$.

To characterize lag synchronization quantitatively, Rosenbulm et al. [33] have introduced the notion of similarity function $S_l(\tau)$ as a time averaged difference between the variables $x_1$ and $x_2$ (with mean values being subtracted) taken with the time shift $\tau$,

$$S_l^2(\tau) = \frac{\langle [x_2(t+\tau) - x_1(t)]^2 \rangle}{\left[\langle x_1^2(t)\rangle \langle x_2^2(t)\rangle\right]^{1/2}}, \tag{B.13}$$

where $\langle x \rangle$ means time average over the variable $x$, and $x_1(t)$ and $x_2(t)$ are the state variables of the drive and response systems, respectively. If the signals $x_1(t)$ and $x_2(t)$ are independent, the difference between them is of the same order as the signals themselves. If $x_1(t) = x_2(t)$, as in the case of complete synchronization, the similarity function reaches a minimum so that $S(\tau) = 0$ for $\tau = 0$. But for the case of nonzero positive value of time shift $\tau$, if $S_l(\tau) = 0$, then there exists a time shift $\tau$ between the two signals $x_1(t)$ and $x_2(t)$ such that $x_2(t) = x_1(t-\tau)$, demonstrating lag synchronization.

We will consider the coupled Rössler systems (B.12) again for illustrative purpose with the same parameters as in the previous section except that the frequency mismatch now is given by $\omega_{1,2} = 0.97 \pm \Delta\omega$ with $\Delta\omega = 0.02$ [33] and the value of the parameter $a$ is chosen as $a = 0.165$. It was noted in the previous section that as the coupling is increased from zero there exists entrainment of phases of the coupled systems in the weak coupling limit. As the coupling strength is increased further one can expect a stronger correlation in the amplitude resulting in the onset

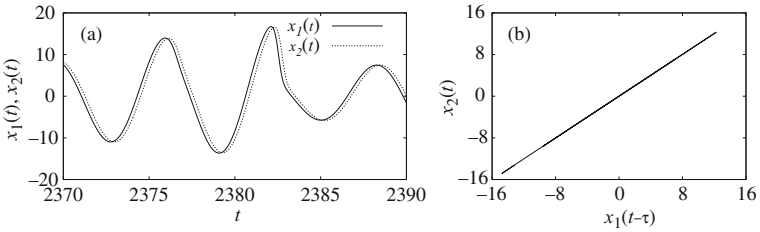


**Fig. B.4** (**a**) Time series plot of the state variables $x_{1,2}$ showing the state of one of the systems evolving with a time lag $\tau = 0.21$ to the state of the other variable for the value of the coupling strength $C = 0.2$ and (**b**) Projection of the attractor of the coupled system on the delayed-coordinates, plot of $x_1(t-\tau)$ Vs $x_2(t)$, demonstrating that the state of one of the oscillators is delayed in time with respect to the other for the above values of the parameters

of lag synchronization for an appropriate value of the coupling strength. In fact, one finds that for $C = 0.2$, the state of one of the oscillators, $x_2$, lags in time to that of the other, $x_1$, with a lag time $\tau = 0.21$ which is illustrated in Fig. B.4a. Projection of the attractor of the coupled system (B.12) on the delayed-coordinate $x_1(t-\tau)$ Vs $x_2(t)$ is shown in Fig. B.4b.

### *B.2.4 Anticipatory Synchronization*

It has also been shown that certain kinds of coupled chaotic systems may synchronize so that the response "anticipates" the driver, $Y(t) = X(t+\tau)$, by synchronizing with the future states. In [36] different unidirectional coupling schemes are considered such as a nonlinear time-delayed feedback either in the driver or in both the coupled systems. The results confirm that the anticipating synchronization can be globally stable due to the interplay between delayed feedback and dissipation, for any relatively small value of the lag time between response and driver. In addition, it has been shown that it is possible to achieve anticipation times larger than the characteristic time scales of the system dynamics, thus introducing a novel way of reducing the unpredictability of chaotic dynamics [37].

Anticipatory synchronization can also be characterized using the same similarity function $S_l(\tau)$ but with a negative time shift $\tau < 0$ instead of the positive time shift $\tau > 0$ in Eq. (B.13). In other words, one may define the similarity function for anticipatory synchronization as

$$S_a^2(\tau) = \frac{\langle [x_1(t-\tau) - x_2(t)]^2 \rangle}{\left[\langle x_1^2(t)\rangle \langle x_2^2(t)\rangle\right]^{1/2}}, \tau < 0 \tag{B.14}$$

Then the minimum of $S_a(\tau)$,that is $S_a(\tau) = 0$, indicates that there exists a time shift $-\tau$ between the two signals $x_1(t)$ and $x_2(t)$ such that $x_2(t) = x_1(t-\tau)$, $\tau < 0$, demonstrating anticipatory synchronization.

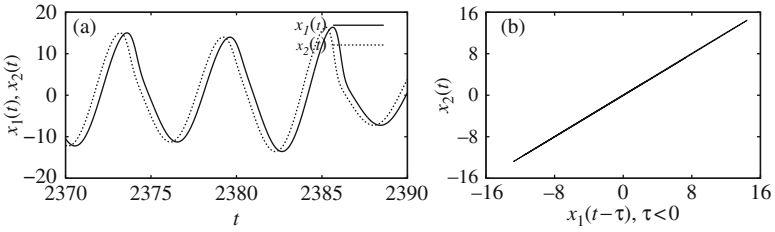


**Fig. B.5** (**a**) Time series plot of the state variables $x_{1,2}$ showing that the drive $x_2(t)$ anticipates the state of the response system $x_1(t)$ with an anticipating time $|\tau| = 0.4$ for the value of the coupling strength $C = 1.0$ and (**b**) Projection of the attractor of the coupled system on the delayed-coordinates, $x_1(t-\tau)$ Vs $x_2(t)$, $\tau < 0$, demonstrating the existence of anticipating synchronization between the drive $x_1(t)$ and response $x_2(t)$ variables

As an illustrative example, we will consider the following unidirectionally coupled Rössler systems [36],

$$\dot{x}_1 = -y_1 - z_1, \tag{B.15a}$$
$$\dot{y}_1 = x_1 + a y_1, \tag{B.15b}$$
$$\dot{z}_1 = 0.2 + z_1(x_1 - 10), \tag{B.15c}$$
$$\dot{x}_2 = -y_2 - z_2 + C(x_1 - x_{2,\tau}), \tag{B.15d}$$
$$\dot{y}_2 = x_2 + a y_2, \tag{B.15e}$$
$$\dot{z}_2 = 0.2 + z_2(x_2 - 10), \tag{B.15f}$$

where the parameter $a$ is fixed as 0.15. It can be easily checked that the above coupled systems exhibit anticipatory synchronization for small values of delay $\tau$ upon increasing the coupling strength. Figure B.5a illustrates that the response $x_2(t)$ anticipates the state of the drive $x_1(t)$ with anticipating time $\tau = 0.4$ for the value of the coupling strength $C = 1.0$ and the projection of the attractor of the coupled system (B.15) on the delayed-coordinates, $x_1(t)$ Vs $x_2(t-\tau)$, is shown in Fig. B.4b.

### *B.2.5 Generalized Synchronization*

In general, completely identical synchronization may not be expected in nonidentical systems because there does not exist an invariant manifold $x = y$. In such cases where there exists an essential difference between the coupled systems, there is no hope to have a trivial manifold in the phase space attracting the system trajectories, and therefore it is not clear at a first glance whether nonidentical chaotic systems can synchronize. However, many works have shown that it is possible to generalize the concept of synchronization to include nonidenticity between the coupled systems and this phenomenon is called *generalized synchronization* [7, 39–41].

In order to define *generalized synchronization* (GS), let us consider the following coupled system

$$\dot{X} = F(X), \tag{B.16a}$$
$$\dot{Y} = G(Y, H_\mu(X)), \tag{B.16b}$$

where $X$ is the n-dimensional state vector of the driver and $Y$ is the m-dimensional state vector of the response. $F$ and $G$ are vector fields, $F : R^n \to R^n$, and $G : R^m \to R^m$. The coupling between the response and the driver is provided by the vector filed $H_\mu(X) : R^n \to R^m$, where the dependence of this function upon the parameters $\mu$ is explicitly considered. When $\mu = 0$, the response system evolves independently of the driver, and we assume that both systems are chaotic.

Some differences in the definition of GS exists in the literature. However, we will discuss here a more general definition given in [39, 40, 72]. When $\mu \neq 0$, the chaotic trajectories of the two systems are said to be synchronized in a generalized sense if there exists a transformation $\psi : X \to Y$ which is able to map asymptotically the trajectories of the driver attractor into the ones of the response attractor $Y(t) = \psi(X(t))$, regardless of the initial condition in the basin of the synchronization manifold $M = (X, Y) : Y = \psi(X)$.

The difference between various definitions of GS is based on the mathematical properties required for the map $\psi$. Reference [67] distinguishes between two types of GS, namely the so-called *weak synchronization* and *strong synchronization*. The latter corresponds to the case of a map $\psi$ which is smooth, in the sense of being differentiable; on the other hand the former corresponds to the case of a map $\psi$ which is non-smooth, in the sense of being not differentiable. Even a stronger version of strong synchronization is considered in [73], called *differentiable generalized synchronization*, requiring continuous differentiability of $\psi$. All of these different approaches have relevant consequences when one looks for the existence of GS in experimental situations. The stability of the manifold $M$ of GS can be determined as in the case of CS, that is, by the negativity of conditional Lyapunov exponents [67] and the use of Lyapunov functions [40].

As an example, we consider the system studied in [74] where the drive system is described by

$$\mu\dot{x}_1 = y_1, \tag{B.17a}$$
$$\mu\dot{y}_1 = -x_1 - \delta y_1 + z_1, \tag{B.17b}$$
$$\mu\dot{z}_1 = \gamma(\alpha_1 f(x_1) - z_1) - \sigma y_1, \tag{B.17c}$$

which is realized in experiments with electrical chaotic circuits [75]. The response system equations are

$$\dot{x}_2 = y_2, \tag{B.18a}$$
$$\dot{y}_2 = -x_2 - \delta y_2 + z_2, \tag{B.18b}$$
$$\dot{z}_2 = \gamma(\alpha_2 f(x_2) - z_2 + g x_1) - \sigma y_2, \tag{B.18c}$$

where $g$ is the coupling strength, and $\gamma = 0.294, \sigma = 1.52, \delta = 0.534$, and $\alpha_2 = 16.7$ are fixed system parameters. The nonlinear function $f(x)$ models the

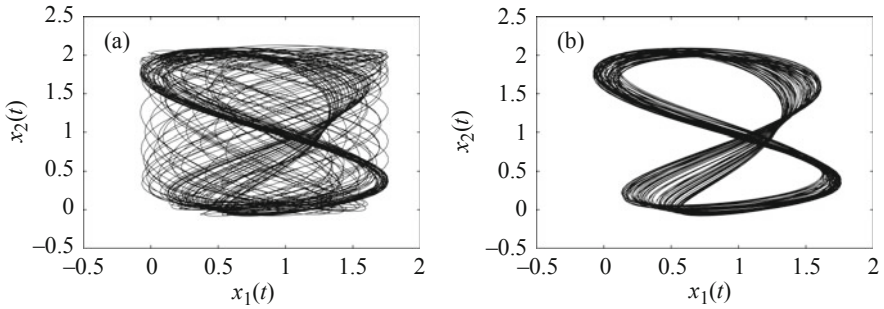


**Fig. B.6** Projection of attractor constructed from the drive (B.17) and response attractors (B.18) and plotted for $(x_1, x_2)$. (**a**) For $\alpha_1 = 15.94$ showing desynchronized state and (**b**) For $\alpha_1 = 15.93$ showing generalized synchronized state

input-output characteristics of a nonlinear converter in the circuit [74, 75]. The parameter $\mu$ in the drive system equations is the time scaling parameter that is used to select the desired frequency ratio of the synchronization. For the parameter values $g = 3.0$, $\mu = 0.498$ and $\alpha_1 = 15.94$ the above systems are in asynchronous state which is shown in Fig. B.6a and as the value of $\alpha$ is decreased to $\alpha = 15.93$ the above systems display generalized synchronization as illustrated in Fig. B.6b.

## References

1. C. Huygens, *Horologium Oscillatorium* (Apud F. Muguet, France, 1673)
2. A.S. Pikovsky, M.G. Rosenblum, J. Kurths, *Synchronization – A Unified Approach to Nonlinear Science* (Cambridge University Press, Cambridge, 2001)
3. E.V. Appleton, Proc. Cambridge Philos. Soc. (Math. Phys. Sci.) **21**, 231 (1922)
4. B. van der Pol, J. van der Mark, Nature **120**, 363 (1927)
5. H. Fujisaka, T. Yamada, Prog. Theor. Phys. **69**, 32 (1983)
6. H. Fujisaka, T. Yamada, Prog. Theor. Phys. **70**, 1240 (1983)
7. V.S. Afraimovich, N.N. Verichev, M.I. Rabinovich, Izvestiya Vysshikh Uchebnykh Zavedenii Radiofizika **29**, 3050 (1986)
8. L.M. Pecora, T.L. Carroll, Phys. Rev. Lett. **64**, 821 (1990)
9. A.S. Pikovsky, Z. Phys. B **55**, 149 (1984)
10. L.M. Pecora, T.L. Carroll, Phys. Rev. A **44**, 2374 (1991)
11. S. Boccaletti, J. Kurths, G. Osipov, D.L. Valladares, C.S. Zhou, Phys. Rep. **366**, 1 (2002)
12. S. Hayes, C. Grebogy, E. Ott, Phys. Rev. Lett. **70**, 3031 (1993)
13. K.M. Cuomo, A.V. Oppenheim, Phys. Rev. Lett. **71**, 65 (1993)
14. T. Kapitaniak, Phys. Rev. E **50**, 1642 (1994)
15. G. Pérez, H.A. Cerdeira, Phys. Rev. Lett. **74**, 1970 (1995)
16. J.H. Peng, E.J. Ding, M. Ding, W. Yang, Phys. Rev. Lett. **76**, 904 (1996)
17. K. Pyragas, Phys. Lett. A **181**, 203 (1993)
18. A. Kittle, K. Pyragas, R. Richter, Phys. Rev. E **50**, 262 (1994)
19. R. Brown, N.F. Rulkov, E.R. Tracy, Phys. Rev. E **49**, 3784 (1994)
20. U. Parlitz, Phys. Rev. Lett. **76**, 1232 (1996)
21. R. He, P.V. Vaidya, Phys. Rev. A **46**, 7387 (1992)
22. R.E. Amritkar, N. Gupte, Phys. Rev. E **47**, 3889 (1993)

23. L. Kocarev, U. Parlitz, Phys. Rev. Lett. **74**, 5028 (1995)
24. U. Parlitz, L. Kocarev, T. Stojanovski, H. Preckel, Phys. Rev. E **53**, 4351 (1996)
25. J. Guemez, M.A. Matias, Phys. Rev. E **52**, R2145 (1995)
26. C.W. Wu, L.O. Chua, Int. J. Bifurcat. Chaos **4**, 979 (1994)
27. E. Ott, C. Grebogi, J.A. Yorke, Phys. Rev. Lett. **64**, 1196 (1990)
28. M. Lakshmanan, K. Murali, *Chaos in Nonlinear Oscillators: Controlling and Synchronization* (World Scientific, Singapore, 1996)
29. M. Lakshmanan, S. Rajasekar, *Nonlinear Dynamics: Integrability, Chaos and Patterns* (Springer, Berlin, 2003)
30. M.G. Rosenblum, A.S. Pikovsky, J. Kurths, Phys. Rev. Lett. **76**, 1804 (1996)
31. T. Yalcinkaya, Y.C. Lai, Phys. Rev. Lett. **79**, 3885 (1997)
32. E.R. Rosa, E. Ott, M.H. Hess, Phys. Rev. Lett. **80**, 1642 (1998)
33. M.G. Rosenblum, A.S. Pikovsky, J. Kurths, Phys. Rev. Lett. **78**, 4193 (1997)
34. S. Rim, I. Kim, P. Kang, Y.J. Park, C.M. Kim, Phys. Rev. E **66**, 015205(R) (2002)
35. M. Zhan, G.W. Wei, C.H. Lai, Phys. Rev. E **65**, 036202 (2002)
36. H.U. Voss, Phys. Rev. E **61**, 5115 (2002)
37. H.U. Voss, Phys. Rev. Lett. **87**, 014102 (2001)
38. C. Masoller, Phys. Rev. Lett. **86**, 2782 (2001)
39. N.F. Rulkov, M.M. Sushchik, L.S. Tsimring, H.D.I. Abarbanel, Phys. Rev. E **51**, 980 (1995)
40. L. Kocarev, U. Parlitz, Phys. Rev. Lett. **76**, 1816 (1996)
41. R. Brown, Phys. Rev. Lett. **81**, 4835 (1998)
42. S. Boccaletti, D.L. Valladares, Phys. Rev. E **62**, 7497 (2000)
43. S. Taherion, Y.C. Lai, Phys. Rev. E **59**, R6247 (1999)
44. D.L. Valladares, S. Boccaletti, Int. J. Bifurcat. Chaos **11**, 2699 (2001)
45. D.V. Senthilkumar, M. Lakshmanan, Chaos **17**, 013112 (2007)
46. A.E. Hramov, A.A. Koronovskii, Europhys. Lett. **79**, 169 (2005)
47. A. Pikovsky, G. Osipov, M. Rosenblum, M. Zaks, J. Kurths, Phys. Rev. Lett. **79**, 47 (1997)
48. A. Pikovsky, M. Zaks, M. Rosenblum, G. Osipov, J. Kurths, Chaos **7**, 680 (1997)
49. K.J. Lee, Y. Kwak, T.K. Lim, Phys. Rev. Lett. **81**, 321 (1998)
50. M.A. Zaks, E.-H. Park, M.G. Rosenblum, J. Kurths, Phys. Rev. Lett. **82**, 4228 (1999)
51. R. Femat, G. Solis-Perales, Phys. Lett. A **262**, 50 (1999)
52. A.E. Hramov, A.A. Koronovskii, Physica D **206**, 252 (2005)
53. I. Fischer, R. Vicente, J. M. Buldu, M. Peil, C.R. Mirasso, M.C. Torrent, J. Garcia-Ojalvo, Phys. Rev. Lett. **97**, 123902 (2006)
54. M. Zhan, Y. Wang, X. Gang, G.W. Wei, C.H. Lai, Phys. Rev. E **68**, 036208 (2003)
55. A. Locquet, F. Rogister, M. Sciamanna, P. Megret, M. Blandel, Phys. Rev. E **64**, 045203(R) (2001)
56. R. Brown, L. Kocarev, Chaos **10**, 344 (2000)
57. S. Boccaletti, L.M. Pecora, A. Pelaez, Phys. Rev. E **63**, 066219 (2001)
58. A.E. Hramov, A.A. Koronovskii, Chaos **14**, 603 (2004)
59. F. Verhulst, *Nonlinear Differential Equations and Dynamical Systems* (Springer, Berlin, Heidelberg, 1990)
60. L. Yu, E. Ott, Q. Chen, Phys. Rev. Lett. **65**, 2935 (1990)
61. D.J. Gauthier, J.C. Bienfang, Phys. Rev. Lett. **77**, 1751 (1996)
62. G. Benettin, C. Froeschlé, H.P. Scheidecker, Phys. Rev. A **19**, 454 (1976)
63. I. Shimada, T. Nagashima, Prog. Theor. Phys. **61**, 1605 (1979)
64. A. Wolf, J.B. Swift, H.L. Swinney, J.A. Vastano, Physica D **16**, 285 (1985)
65. J.L. Willems, *Stability Theory of Dynamical Systems* (Wiley, New York, 1970)
66. K. Murali, M. Lakshmanan, Phys. Rev. E **49**, 4882 (1994)
67. K. Pyragas, Phys. Rev. E **54**, R4508 (1996)
68. C. Sparrow, *The Lorenz Equations, Bifurcations, Chaos, and Strange Attractors*, (Springer, New York, 1982)
69. G.V. Osipov, A.S. Pikovsky, M.G. Rosenblum, J. Kurths, Phys. Rev. E **55**, 2353 (1997)

70. D. Gabor, J. IEE London **93**, 429 (1946)
71. O.E. Rössler, Phys. Let. A **57**, 397 (1976)
72. H.D.I. Abarbanel, N.F. Rulkov, M.M. Sushchik, Phys. Rev. E **53**, 4528 (1996)
73. B.R. Hunt, E. Ott, J.A. Yorke, Phys. Rev. E **55**, 4029 (1997)
74. N.F. Rulkov, C.T. Lewis, Phys. Rev. E **63**, 065204(R) (2001)
75. N.F. Rulkov, Chaos **6**, 262 (1996)

# Appendix C
# Recurrence Analysis

## C.1 Introduction

The concept of recurrence dates back to Poincaré [1], who proved that after a sufficiently long time the trajectory of a chaotic system in phase space will return arbitrarily close to any former point of its path with probability one. However, the concept of recurrence within the framework of chaotic systems was not considered until the sixties, when the now famous Lorenz equation was derived by E. Lorenz as a simplified equation of convection rolls [2, 3]. Later in 1987, Eckmann et al. introduced the method of recurrence plots (RPs), a technique that visualizes the recurrences of a dynamical system and gives information about the behavior of its trajectory in phase space [4]. This technique has become popular in the last decade because of its applicability to rather short and non-stationary time series. Further, cross recurrence plots (CRPs) (a bivariate extension of the RP) was introduced by Zbilut et al. [5] and Marwan and Kurths [6] to analyse the dependencies between two different systems by comparing their states [5, 6]. As an extension of CRPs to analyse physically different systems with different phase space dimensions, joint recurrence plots (JRPs) were introduced. Also, in order to go beyond the visual inspection of RPs, several measures of complexity which quantify the small scale structures in RPs have been proposed [7–10] and are known as recurrence quantification analysis (RQA). These measures are based on the recurrence point density and the diagonal and vertical line structures of the RP. Furthermore, a more theoretical study of the relationship between RPs and the properties of dynamical systems has also been addressed [10–15]. The concept of recurrence plots and its measures have been applied in numerous fields of research including astrophysics [16, 17], earth sciences [18–20], engineering [21, 22], biology [23, 24] and cardiology/neuroscience [25–28]. In the following, we describe briefly the concept of recurrence plots along with CRP and JRP. We will also discuss the various quantification measures introduced to characterize synchronization transitions in coupled chaotic systems.

## C.2 Recurrence Plots and Their Variants

In this section, we will describe briefly the concept of recurrence plots and their variants such as cross recurrence plots and joint recurrence plots to analyse the data of different physical systems of same or even different dimensions along with suitable illustrations.

### *C.2.1 Recurrence Plots*

As mentioned in the introduction, RPs provide a visual impression of the trajectory of a dynamical system in phase space. Suppose that the time series $\{X_i\}_{i=1}^{N}$ representing the trajectory of a system in phase space is given, with $X_i \in \mathbb{R}^d$. The RP efficiently visualises recurrences and can be formally expressed by the matrix

$$\mathbb{R}_{i,j} = \Theta(\varepsilon - ||X_i - X_j||), \qquad i, j = 1, \cdots, N, \tag{C.1}$$

where $N$ is the number of measured points $X_i$, $\varepsilon$ is a predefined threshold, $\Theta$ is the Heaviside function (i.e. $\Theta(x) = 0$, if $x < 0$, and $\Theta(x) = 1$ otherwise) and $||.||$ is the Euclidean norm. For $\varepsilon$-recurrent states, that is for states which are in an $\varepsilon$-neighbourhood, we have the following notion:

$$X_i \approx X_j \Longleftrightarrow \mathbb{R}_{i,j} \equiv 1. \tag{C.2}$$

The graphical representation of the matrix $\mathbb{R}_{i,j}$ is called recurrence plot (RP). The RP is obtained by plotting the recurrence matrix, Eq. (C.1), using different colors for its binary entries, for example by marking a black dot at the coordinates $(i, j)$, if $\mathbb{R}_{i,j} \equiv 1$, and a white dot, if $\mathbb{R}_{i,j} \equiv 0$. Since $\mathbb{R}_{i,i} \equiv 1 \; |_{i=1}^{N}$ by definition, the RP has always a black main diagonal line. Furthermore, the RP is symmetric by definition with respect to the main diagonal, that is $\mathbb{R}_{i,j} \equiv \mathbb{R}_{j,i}$.

A crucial parameter of an RP is the threshold $\varepsilon$. Therefore, special attention has to be required for its choice. If $\varepsilon$ is chosen too small, there may be almost no recurrence points and we cannot learn anything about the recurrence structure of the underlying system. On the other hand, if $\varepsilon$ is chosen too large, almost every point is a neighbour of every other point, which leads to a lot of artefacts. A too large $\varepsilon$ includes also points into the neighbourhood which are simple consecutive points on the trajectory. Hence, one has to find an appropriate value for $\varepsilon$. Moreover, the influence of noise can entail choosing a larger threshold, because noise would distort any existing structure in the RP [10].

Several methods have been advocated in the literature to estimate the value of threshold $\varepsilon$ with their own advantages and disadvantages which has been discussed in [10]. Among them, we use the approach that preserves the fixed recurrence point density. In order to find an $\varepsilon$ which corresponds to a fixed recurrence point density or recurrence rate (RR) defined as

$$RR(\varepsilon) = \frac{1}{N^2} \sum_{i,j=1}^{N} \mathbb{R}_{i,j}(\varepsilon), \tag{C.3}$$

the cumulative distribution of the $N^2$ distances between each pair of vectors can be used. The $RR$th percentile is then the required $\varepsilon$. An alternative is to fix the number of neighbours for every point of the trajectory. In this case, the threshold is actually different for each point of the trajectory. The advantage of these two methods is that both of them preserve the recurrence point density and allow one to compare RPs of different systems without the necessity of normalising the time series beforehand. Nevertheless, the choice of $\varepsilon$ depends strongly on the system under study.

For illustration, we will show the RPs of three different motions, namely (i) of a periodic motion on a circle (Fig. C.1a), (ii) of a chaotic attractor of Rössler system (Fig. C.1b) and (iii) of a Gaussian white noise (Fig. C.1c). In all our simulation, we have chosen the threshold value for $\varepsilon$ as $\varepsilon = 0.03RR$ and the sampling interval to be $\Delta t = 0.1$. The RP of the purely periodic oscillation shown in Fig. C.1a consists of uninterrupted diagonal lines separated by the distance $T$, where $T$ is the period of the oscillation. This is due to the fact that the position of the system in the phase space recurs exactly at the same point after a cycle and hence one has identical recurrence. The RP of Gaussian white noise depicted in Fig. C.1c is rather homogeneous, consisting of mainly single points, indicating the randomness of its behavior. The RP of chaotic attractor of Rössler system is illustrated in Fig. C.1b, which shows that the predominant structures are intermediate between that of periodic oscillations and that of purely stochastic motions. The RP of Rössler attractor also shows diagonal lines which are shorter (interrupted) and the vertical distance between the diagonal lines is not constant because of the multiple time scales of the chaotic system. The interrupted diagonal lines are due to the exponential divergence of nearby trajectories (sensitive to slightly different initial conditions). However, on the upper right of Fig. C.1b, there is a small rectangular patch which rather looks like the RP of the periodic motion and this structure corresponds to an unstable periodic orbit of the Rössler attractor [10]. It is also conjectured that shorter the diagonals in the RP, the less the predictability of the system [29], and indeed it was suggested that the inverse of the longest diagonal (except the main diagonal for which $i = j$) is proportional to the largest Lyapunov exponent of the system by Eckmann et al. [4].

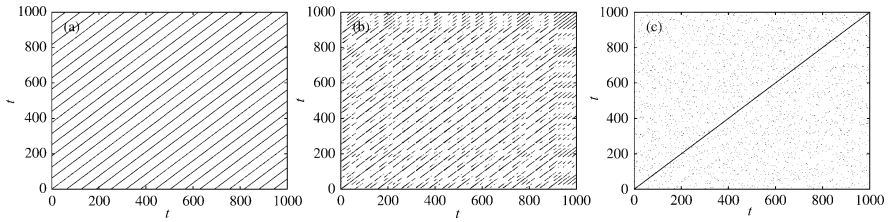


**Fig. C.1** Recurrence Plots of (**a**) a periodic oscillation, (**b**) a chaotic attractor of Rössler system and (**c**) a Gaussian white noise

### C.2.2 Cross Recurrence Plots (CRP)

As mentioned in the introduction, CRP is a bivariate extension of the RP and was introduced to analyse the difference between two different systems [5, 6]. CRPs can be regarded as a generalisation of the linear cross-correlation function [10]. The cross recurrence matrix, analogous to RP, of two dynamical systems represented by the trajectories $X$ and $Y$ in a $d$-dimensional phase space is defined by

$$CR_{i,j}^{X,Y} = \Theta(\varepsilon - ||X_i - Y_j||), \qquad i = 1, \cdots, N, \qquad j = 1, \cdots, M, \quad \text{(C.4)}$$

where $N$ and $M$ are the lengths of the trajectories $X$ and $Y$, respectively. Note that $N$ may not be equal to $M$ and hence the matrix $CR$ is not necessarily a square matrix. As a CRP is plotted for those times when a state of the first system recurs to that of the other system, both the systems are represented in the same phase space. The components of $X_i$ and $Y_i$ are usually normalised before computing the cross recurrence matrix, while the other possibilities are to use the fixed amount of neighbours for each $X_i$ in which case the components need not be normalised. It has been shown that the latter choice of the fixed neighborhood has the additional advantage of suitability for slowly changing trajectories [10].

As an illustration, the CRP of the coupled Rössler systems (Eq. (B.12)) for the same value of the parameters as in Sect. B.2.2 and for the value of the coupling strength $C = 0.01$ is shown in Fig. C.2. As the values of the main diagonal $CR_{i,i}$ are not necessarily unity, CRPs do not have a black main diagonal line as in RPs as in Fig. C.2. It has been shown that measures based on the length of the diagonally oriented lines are used to find the nonlinear interactions between two systems, which cannot be detected by the common cross-correlation function [6, 10]. An important property of CRPs is that they reveal the local difference of the dynamical evolution of close trajectory segments, represented by bowed lines. A time dilation or time compression of one of the trajectories causes a distortion of the diagonal lines. For

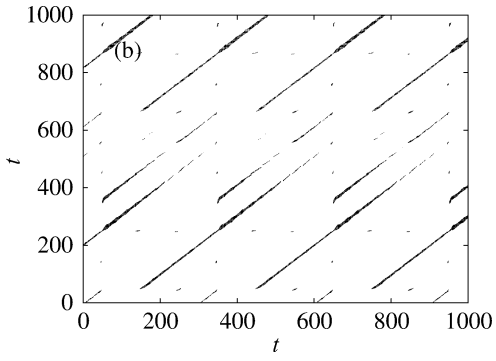


**Fig. C.2** Cross recurrence plot of the coupled Rössler systems (Eq. (B.12)) for the same value of the parameters as in Sect. B.2.2 and for the value of the coupling strength $C = 0.01$

two identical trajectories, the CRP is the RP of a single trajectory and contains the main black diagonal line.

### C.2.3 Joint Recurrence Plots (JRP)

We have seen above that CRP can be used to analyse the interrelation between two different systems. However, CRP cannot be used to analyse two physically different systems because the two different physical units or different phase space dimensions do not make sense in computing CRP. A different possibility to compare the states of different systems is to consider the recurrences of their trajectories in their corresponding phase spaces separately and then look for the times when both of them recur simultaneously, that is when joint recurrence occurs. The individual phase spaces are preserved by this approach and different thresholds for each system $\varepsilon^X$ and $\varepsilon^Y$ are considered, in respect of the natural measure of both the systems. Joint recurrence matrix for two systems $X$ and $Y$ can be defined as

$$JR_{i,j}^{X,Y}(\varepsilon^X, \varepsilon^Y) = \Theta(\varepsilon^X - ||X_i - X_j||)\Theta(\varepsilon^Y - ||Y_i - Y_j||), \qquad i, j = 1, \cdots, N. \tag{C.5}$$

JRP of the coupled Rössler systems (Eq. (B.12)) for the same value of the parameters as in Sect. B.2.2 and for the value of the coupling strength $C = 0.01$ is shown in Fig. C.3.

The bivariate joint recurrence plot can be generalized to analyse $n$ systems $(X_{(1)}, X_{(2)}, ..., X_{(n)})$ by using multivariate joint recurrence matrix, which can be represented using Eq. (C.1) as

$$JR_{i,j}^{X_{(1,2,...,n)}}(\varepsilon^{X_{(1)}}, ..., \varepsilon^{X_{(n)}}) = \prod_{k=1}^{n} \mathbb{R}_{i,j}^{X_{(k)}}(\varepsilon^{X_{(k)}}), i, j = 1, \cdots, N. \tag{C.6}$$

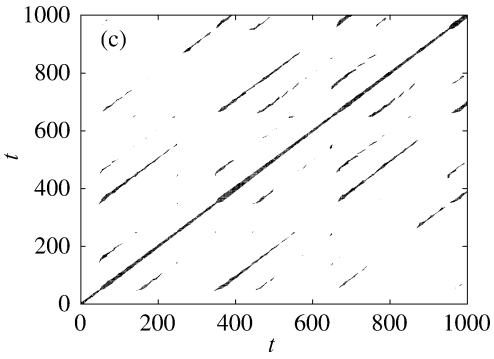


**Fig. C.3** Joint recurrence plot of the coupled Rössler systems (Eq. (B.12)) for the same value of the parameters as in Sect. B.2.2 and for the value of the coupling strength $C = 0.01$

In addition, a delayed version of the joint recurrence matrix can also be introduced as

$$JR_{i,j}^{X,Y}(\varepsilon^X, \varepsilon^Y, \tau) = \mathbb{R}_{i,j}^{X}(\varepsilon^X)\mathbb{R}_{i+\tau,j+\tau}^{Y}(\varepsilon^Y), \qquad i, j = 1, \cdots, N-\tau, \quad \text{(C.7)}$$

to analyse the interacting delayed systems [10]. JRP is invariant under permutation of the coordinates in one or more of the systems. It can also be computed using a fixed amount of nearest neighbours. In this case, each RPs which contributes to the JRP is computed using the same number of nearest neighbours. These RPs obtained from CRP, JRP and their variants are exploited in quantifying several dynamical properties and their transitions using recurrence quantification analysis as discussed in the next section.

## C.3 Recurrence Quantification Analysis (RQA)

Several measures of complexity which quantify the small scale structures in RPs have been proposed and are known as recurrence quantification analysis. These measures are based on the recurrence point density, the diagonal and vertical line structures of the RP. Studies based on RQA measures show that they are able to identify bifurcation points, including chaos-order and chaos-chaos transitions [10]. Several recurrence quantification measures have been introduced for different requirements. Some of the most important measures include Recurrence Rate (RR), Determinism ($DET$), Divergence ($DIV$), Entropy ($ENTR$), Trend ($TREND$), Ratio ($RATIO$), Linearity ($LAM$), Trapping Time ($TT$), Maximal vertical length ($V_{max}$), etc. It has also been shown that several dynamical invariants such as correlation entropy, correlation dimension, generalized mutual information, etc can also be calculated using RQA. Detailed discussion on all of the above RQAs can be found in [10] and, all of the methods and procedure discribed in this appendix are available in the CRP toolbox for Matlab (Provided by TOCSY: http://tocsy.agnld.uni-potsdam.de). However, in the following, we will focus our discussion on some of the RQAs that have been introduced to characterize and to identify different kinds of synchronization transitions in coupled chaotic systems.

### *C.3.1 Generalized Autocorrelation Function, $P(t)$*

Generalized autocorrelation function $P(t)$ has been defined as [10, 30]

$$P(t) = \frac{1}{N-t}\sum_{i=1}^{N-t}\Theta(\varepsilon - ||X_i - X_{i+t}||). \quad \text{(C.8)}$$

If any two coupled oscillators are in phase synchronization (PS), then the distances between the diagonal lines in their respective RPs coincide as their phases, and

hence their time scales are locked to each other. As PS is characterized by entrainment in the phases of the interacting systems while their amplitudes remain uncorrelated, their respective RPs remain non-identical. However, if the probability that the first oscillator recurs after $t$ time steps is high, then the probability that the second oscillator recurs after the same time interval is also high, and vice versa. Therefore, looking at the probability $P(t)$ that the system recurs to the $\varepsilon$ neighborhood of a former point of the trajectory $X$ after $t$ time steps and comparing $P(t)$ of both the system allows to detect and quantify PS.

Generalized autocorrelation function $P(t)$ can be considered as a statistical measure about how often the phase $\phi$ has increased by $2\pi$ or multiples of $2\pi$ within the time $t$ in the original space. If two systems are in a phase synchronized state, their phases increase on the average by $K.2\pi$, where $K$ is a natural number, within the same time interval $t$. The value of $K$ corresponds to the number of cycles when $||X(t+T) - X(t)|| \sim 0$, or equivalently when $||X(t+T) - X(t)|| < \varepsilon$, where $T$ is the period of the system. Hence, looking at the coincidence of the positions of the maxima of $P(t)$ for both the systems, one can qualitatively identify CPS. It is to be noted that the heights of the local maxima are in general different for both systems if they are only in PS.

### *C.3.2 Correlation of Probability of Recurrence (CPR)*

A criterion to quantify phase synchronization between two systems is the cross correlation coefficient between $P_1(t)$ and $P_2(t)$ ($P_1(t)$ represents the probability of recurrence of the first system and $P_2(t)$ that of the second system) which can be defined as Correlation of Probability of Recurrence (CPR)

$$CPR = \langle \bar{P}_1(t)\bar{P}_2(t)\rangle / \sigma_1\sigma_2, \tag{C.9}$$

where $\bar{P}_{1,2}$ means that the mean value has been subtracted and $\sigma_{1,2}$ are the standard deviations of $P_1(t)$ and $P_2(t)$, respectively. If both systems are in CPS, the probability of recurrence is maximal at the same time $t$ and CPR $\approx 1$. If they are not in CPS, the maxima do not occur simultaneously and hence one can expect a drift in both the probability of recurrences and low values of CPR.

It has also shown that this method is highly efficient even for non-phase coherent oscillators and it is able to detect PS even in time series which are strongly corrupted by noise. One of the most important applications of this method is that it can also be applied to experimental time series with noise.

### *C.3.3 Joint Probability of Recurrence (JPR)*

Joint probability of recurrence to quantify the existence of generalized synchronization (GS) between two systems is defined as

$$JPR = \frac{S - RR}{1 - RR}, \tag{C.10}$$

where, $S = \frac{RR_{1,2}}{RR}$, $RR_{1,2}$ is the recurrence rate of the JRP of both the systems and $RR_1 = RR_2 = RR$ is the recurrence rate of the individual systems.

### *C.3.4 Similarity of Probability of Recurrence (SPR)*

As the recurrence matrix contains only information about the neighborhood of each point of a time series, the RPs of systems in GS must be almost identical. Hence, it follows that their respective probabilities of recurrence must coincide and this suggests the similarity coefficient between $P_1(t)$ and $P_2(t)$ represented as

$$SPR = 1 - \langle (\bar{P}_1(t) - \bar{P}_2(t))^2 \rangle / \sigma_1 \sigma_2, \tag{C.11}$$

is of order 1 if both systems are in GS and approximately zero or negative if they evolve independently.

## C.4 Synchronization and Recurrences

In this section, we will investigate the onset, existence and transition among different kinds of synchronizations by using recurrence plots and recurrence quantification analysis discussed above. It may be noted that these indices based on the recurrence are of considerable importance in synchronization analysis of experimental systems and, in particular, in the case of very small available data set. With these indices, one can quantify the degree of synchronization in complex interacting systems, specifically in the case of non-coherent attractors. These methods are more appropriate for non-stationary data. In the following, we will analyse (i) phase synchronization in mutually coupled Rössler systems [31] and (ii) transition from phase to lag synchronization again in mutually coupled Rössler systems [32] but in slightly different parameter regimes using recurrence plots and recurrence indices discussed above.

### *C.4.1 PS in Mutually Coupled Rössler Systems*

Phase synchronization has already been discussed in detail in Sect. B.2.2 and it has been illustrated using mutually coupled Rössler systems [31]. Now, we will discuss about the structure of recurrence plots, the nature of generalized autocorrelation function, $P(t)$, and correlation of probability of recurrence, CPR, for two different values of the coupling strength corresponding to non-synchronized and phase synchronized state in these systems. It is well known that PS is characterized by

entrainment in the phase of the interacting systems while their amplitudes remain uncorrelated. During PS, the phases get locked and so also the frequencies. Therefore, the recurrence plots of both the systems have the same distance (vertical) between the diagonal lines, which corresponds to the period of oscillation, while their respective RPs remain nonidentical.

Recurrence plot of both of the mutually coupled Rössler systems (Eq. (B.12)) for the same values of the parameters as in Sect. B.2.2 are shown in Fig. C.4a, b, respectively, for the value of coupling strength $C = 0.01$ in the non-synchronized regime. The generalized autocorrelation functions, $P_{1,2}(t)$ of both the systems are shown in Fig. C.4c, which indicates that the positions of local maxima are not in coincidence and there exists a drift between them indicating non-synchronized state. The value of correlation of probability of recurrence, $CPR = 0.022$, is rather low confirming the non-synchronized state. Similarly, RPs of both the systems are shown in Fig. C.5a, b, respectively, for the value of coupling strength $C = 0.035$ corresponding to PS regime. Now both $P_1(t)$ and $P_2(t)$ are in perfect coincidence in their positions of local maxima indicating PS (Fig. C.5c). In addition, the value of the correlation coefficient $CPR = 0.91$ which is rather high, indicating a high degree of PS.

The transition from non-synchronized state to PS and the onset of PS can also be clearly revealed by the index $CPR$. It has been demonstrated [31] that the onset of PS occurs at the value of coupling strength $C = 0.027$ and PS exists for values $C > 0.027$ as indicated by the Lyapunov exponents shown in Fig. C.6a in the range of coupling strength $C \in (0, 0.04)$. The onset of PS at this value is also clearly revealed

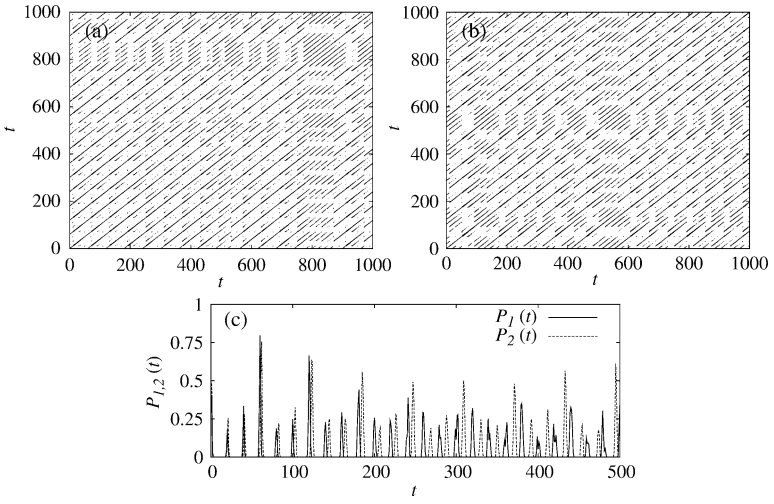


**Fig. C.4** Recurrence plots of the coupled Rössler systems (Eq. (B.12)) for the same value of the parameters as in Sect. B.2.2 but for the value of the coupling strength $C = 0.01$ in the non-synchronized state. (**a**) First system, (**b**) Second system and (**c**) Generalized autocorrelation functions, $P_{1,2}(t)$, of both the systems

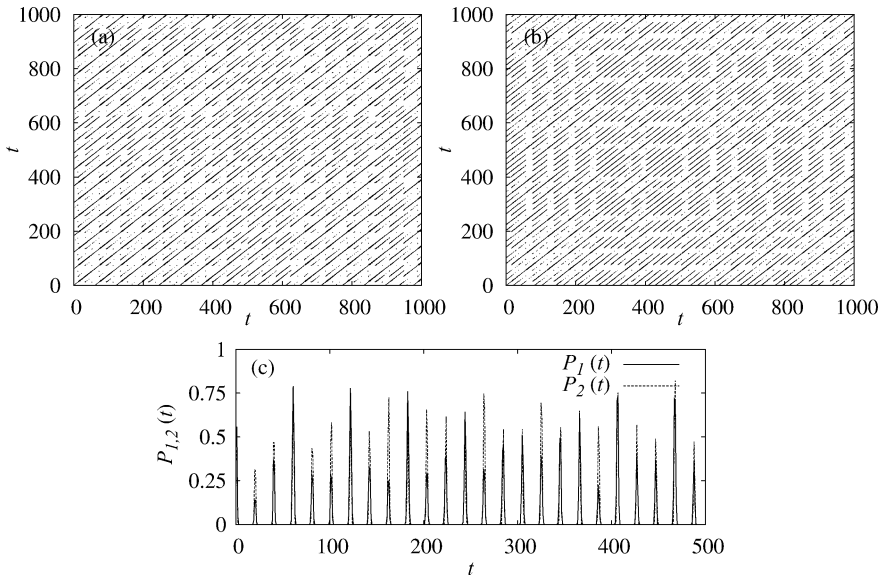


**Fig. C.5** Recurrence plots of the coupled Rössler systems (Eq. (B.12)) for the same value of the parameters as in Sect. B.2.2 but for the value of the coupling strength $C = 0.035$ in the PS state. (**a**) First system, (**b**) Second system and (**c**) Generalized autocorrelation functions, $P_{1,2}(t)$, of both the systems

by the index *CPR* shown in Fig. C.6b in the same range of the coupling strength $C$ of the mutually coupled Rössler systems (Eq. (B.12)). The value of the *CPR* shows a sudden increase in its value at $C = 0.027$ and above this value of coupling strength *CPR* fluctuates near to but less than unity characterizing the degree of PS.

### *C.4.2 Phase to Lag Synchronization*

Lag synchronization (LS) has also been already discussed in Sect. B.2.3, along with an illustration as demonstrated in [32]. With the same values of parameters as discussed in Sect. B.2.3 for mutually coupled Rössler systems (Eq. (B.12)), we will characterize the transition from non-synchronized state to PS and then to an LS state using the recurrence indices. As LS is a special case of generalized synchronization (GS) all the discussion for LS will also hold for GS.

Since RPs and generalized autocorrelation functions for both the coupled systems are already shown in the non synchronized and PS regimes, we concentrate here on LS only. RPs and $P_{1,2}(t)$ of the mutually coupled Rössler systems (Eq. (B.12)) for

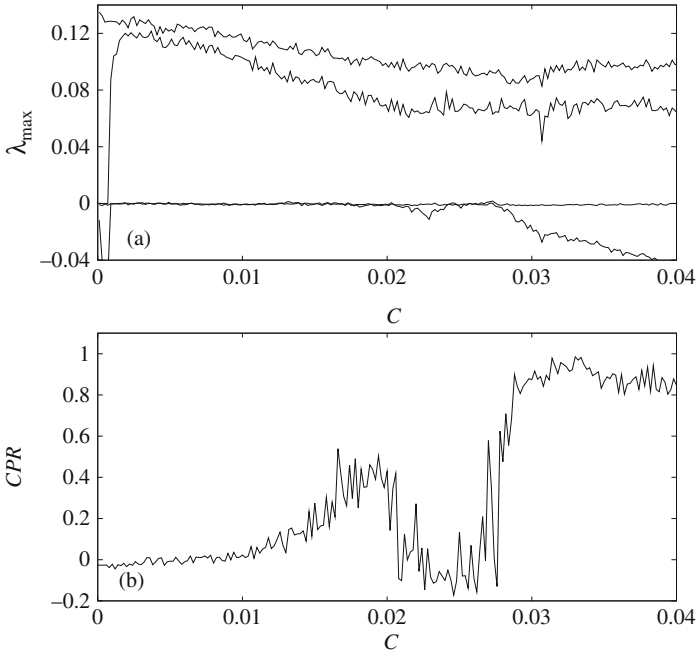


**Fig. C.6** (**a**) Four largest Lyapunov exponents in the range of coupling strength $C \in (0, 0.04)$ of the mutually coupled Rössler systems (Eq. (B.12)) studied in Sect. B.2.2 and (**b**) Correlation of probability of recurrence, *CPR*, in the same range of the coupling strength characterizing the onset of PS

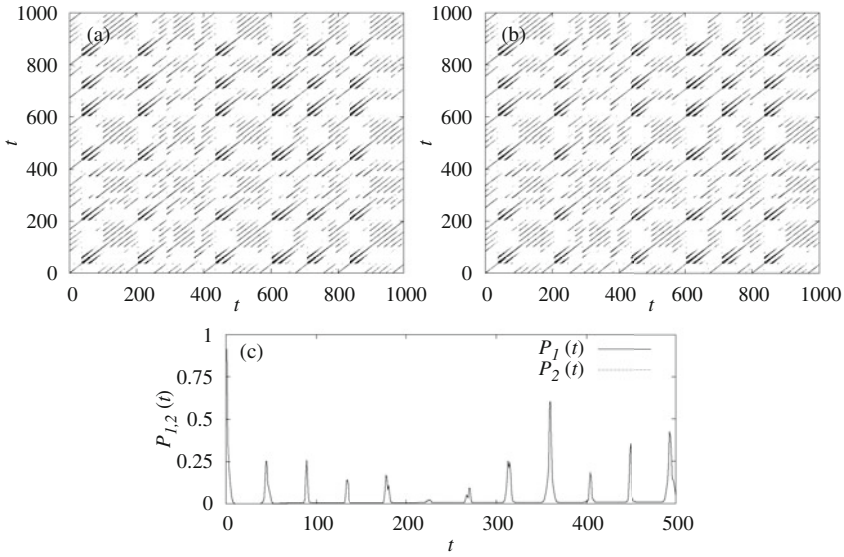


**Fig. C.7** Recurrence plots of the coupled Rössler systems (Eq. (B.12)) for the same value of the parameters as in Sect. B.2.3 and for the value of the coupling strength $C = 0.2$ in the LS state. (**a**) First system, (**b**) Second system and (**c**) Generalized autocorrelation functions, $P_{1,2}(t)$, of both the systems

the value of coupling strength $C = 0.2$ is shown in Fig. C.7, where both the systems are in LS. It is evident that the RPs of both the systems are identical confirming the existence of lag (generalized) synchronization between the coupled systems. Furthermore, the generalized autocorrelation functions, $P_{1,2}(t)$, are also in perfect coincidence both with their positions and with their amplitudes confirming the existence of lag (generalized) synchronization. Correspondingly, the value of the indices $CPR = 0.881$ and $SPR = 0.999$ are rather high attributing to the degree of LS.

Transition from the non-synchronized state to PS and then from PS to LS in mutually coupled Rössler systems has been demonstrated in [32]. It has been shown that the onset of PS occurs at the critical value of the coupling strength $C_p = 0.036$ and that of LS occurs at $C_l = 0.14$ as indicated by the largest Lyapunov exponents of the coupled Rössler systems shown in Fig. C.8a. Indices *CPR*, *JPR*, *SPR* are depicted in Fig. C.8b in the range of coupling strength $C \in (0, 0.2)$. Indices *CPR* and *SPR* indicate the onset of PS at the critical value of the coupling strength $C_p = 0.036$ as indicated by the Lyapunov exponents, by a sudden increase in their values. The onset of LS in the coupled Rössler systems is also indicated by the indices *JPR* and *SPR* exactly at the same critical value of the coupling strength $C_l = 0.14$ by saturation in their amplitudes at high values near to unity.

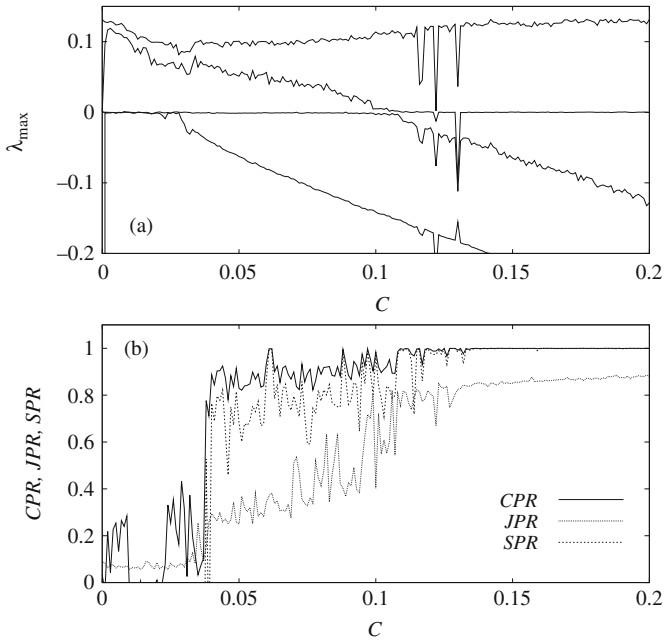


**Fig. C.8** (**a**) Four largest Lyapunov exponents in the range of coupling strength $C \in (0, 0.2)$ of the mutually coupled Rössler systems (Eq. (B.12)) studied in Sect. B.2.3 and (**b**) Indices, *CPR*, *JPR*, *SPR*, in the same range of the coupling strength characterizing the onset of PS, LS and transition among them

## References


1. H. Poincaré, Acta Mathematica **13**, 1 (1890)
2. E.N. Lorenz, J. Atmos. Sci. **20**, 130 (1963)
3. E.N. Lorenz, J. Atmos. Sci. **26**, 636 (1969)
4. J.-P. Eckmann, S.O. Kamphorst, D. Ruelle, Europhys. Lett. **5**, 973 (1987)
5. J.P. Zbilut, A. Giuliani, C.L. Webber Jr., Phys. Lett. A **246**, 122 (1998)
6. N. Marwan, J. Kurths, Phys. Lett. A **302**, 299 (2002)
7. J.P. Zbilut, C.L. Webber Jr., Phys. Lett. A **171**, 199 (1992)
8. C.L. Webber Jr., J.P. Zbilut, J. Appl. Physiol. **76**, 965 (1994)
9. N. Marwan, N. Wessel, U. Meyerfeldt, A. Schirdewan, J. Kurths, Phys. Rev. E **66**, 026702 (2002)
10. N. Marwan, M.C. Romano, M. Thiel, J. Kurths, Phys. Rep. **438**, 237 (2007)
11. M.C. Casdagli, Physica D **108**, 12 (1997)
12. P. Faure, H. Korn, Physica D **122**, 265 (1998)
13. J. Gao, H. Cai, Phys. Lett. A **270**, 75 (1999)
14. M. Thiel, M.C. Romano, J. Kurths, R. Meucci, E. Allaria, T. Arecchi, Physica D **171**, 138 (2002)
15. M. Thiel, M.C. Romano, P. Read, J. Kurths, Chaos **14**, 234 (2004)
16. J. Kurths, U. Schwarz, C.P. Sonett, U. Parlitz, Nonlinear Processes Geophys. **1**, 72 (1994)
17. N.V. Zolotova, D.I. Ponyavin, Astron. Astrophys. **499**, L1 (2006)
18. N. Marwan, M. Thiel, N.R. Nowaczyk, Nonlinear Processes Geophys. **9**, 325 (2002)
19. N. Marwan, M.H. Taruth, M. Vuille, J. Kurths, Clim. Dyn. **21**, 317 (2003)
20. T.K. March, S.C. Chapmann, R.O. Dendy, Physica D **200**, 171 (2005)
21. A.S. Elwakil, A.M. Soliman, Chaos Solit. Fract. **10**, 1399 (1999)
22. J.M. Nichols, S.T. Trickey, M. Seaver, Mech. Syst. Signal Process. **20**, 421 (2006)
23. A. Giuliani, C. Manetti, Phys. Rev. E **53**, 6336 (1996)
24. C. Manetti, A. Giuliani, M.A. Ceruso, C. L. Webber Jr., J. P. Zbilut, Phys. Lett. A **281**, 317 (2001)
25. J.E. Naschitz, I. Rosner, M. Rozenbaum, M. Fields H. Isseroff, J.P. Babich, E. Zuckerman, N. Elias, D. Yeshurun, S. Naschitz, E. Sabo , QJM:Int. J. Med. **97**, 141 (2004)
26. N. Thomasson, T.J. Hoeppner, C.L. Webber Jr., J.P. Zbilut, Phys. Lett. A **279**, 94 (2001)
27. N. Marwan, A. Meinke, Int. J. Bifurcat. Chaos **14**, 761 (2004)
28. U.R. Acharya, O. Faustand, N. Kannathal, T.L. Chua, S. Laxminarayan, Comput. Meth. Prog. Biomed. **80**, 37 (2005)
29. F.M. Atay, Y. Altintas, Phys. Rev. E **59**, 6 (1999)
30. M.C. Romano, M. Thiel, J. Kurths, I.Z. Kiss, J.L. Hudson, Europhys. Lett. **71**, 466 (2005)
31. M.G. Rosenblum, A.S. Pikovsky, J. Kurths, Phys. Rev. Lett. **76**, 1804 (1996)
32. M.G. Rosenblum, A.S. Pikovsky, J. Kurths, Phys. Rev. Lett. **78**, 4193 (1997)

# Appendix D
# Some More Examples of DDEs

## D.1 Introduction

In addition to the examples of different kinds of DDEs presented in Chap. 1 and other chapters, we will describe briefly some of the available DDEs of various forms that have been used in the literature in different areas of science and technology.

## D.2 DDEs with Constant Delay

DDEs with constant delays have been discussed in Sect. 1.1.1 of Chap. 1 along with some of the instances where they appear. In the following we will present few more of them briefly.

### *D.2.1 Hutchinson's Equation/Delayed Logistic Equation*

Hutchinson [1, 2] proposed a more realistic logistic delay equation for single species dynamics by assuming egg formation to occur $\tau$ time units before hatching represented as follows,

$$\frac{dx}{dt} = rx(t)\left[1 - \frac{x(t-\tau)}{K}\right], \tag{D.1}$$

where $x(t)$ denotes the population size at time $t$, $r > 0$ is the intrinsic growth rate and $K > 0$ is the carrying capacity of the population. This equation is often referred to as the *Hutchinson's equation or delayed logistic equation.*

### *D.2.2 Gopalsamy and Ladas Population Model*

Gopalsamy and Ladas [3] proposed a single species population model exhibiting the Allee effect in which the per capita growth rate is a quadratic function of the density and is subject to more than one identical time-delay terms represented as

$$\frac{dx}{dt} = x(t)\left[a + bx(t-\tau) - cx^2(t-\tau)\right], \tag{D.2}$$

where $a > 0, c > 0, \tau > 0$ and $b$ are real constants. In this model, when the density of the population is not small, the positive feedback effects of aggregation and cooperation are dominated by density-dependent stabilizing negative feedback effects due to intraspecific competition. In other words, intraspecific mutualism dominates at low densities and intraspecific competition dominates at higher densities [2, 3].

### *D.2.3 Stem-Cell Model*

The dynamics of pluripotential stem-cell population is governed by the pair of coupled DDEs [4, 5]

$$\frac{dx}{dt} = -\gamma x(t) + \beta x(t)^2 - exp(-\gamma\tau)\beta y_\tau^2, \tag{D.3}$$

$$\frac{dy}{dt} = -\left[\beta y(t) + \delta\right] y(t) + 2exp(-\gamma\tau)\beta y_\tau^2, \quad y_\tau = y(t-\tau), \tag{D.4}$$

where $\tau$ is the time required for a cell to traverse the proliferative phase and $\beta$ is the resting to proliferative phase feedback rate. Further details can be found in [4, 5].

### *D.2.4 Pupil Cycling Model*

Pupil cycling is described by the following DDE with piecewise constant negative feedback

$$\frac{dx}{dt} = y(t), \tag{D.5}$$

$$\frac{dy}{dt} = f(x_\tau), \qquad x_\tau = x(t-\tau), \tag{D.6}$$

where the piecewise constant negative feedback is given as

$$f(x) = \begin{cases} a, & x > \theta \\ b, & x \le \theta. \end{cases} \tag{D.7}$$

Here $x(t)$ is the pupil area at time $t$, $\tau$ is the time-delay, $a, b$ describe retinal illumination ($a > b$) and $\theta$ is a threshold area [6, 7].

## D.3 DDEs with Discrete Delays

Given the general form of DDEs with discrete delays as in Sect. 1.1.2 along with suitable examples, we will describe here some other examples of discrete/multiple delays with their explicit equations and their details.

### *D.3.1 Australian Blowfly Model*

Braddock and van den Driessche [2, 3, 8] proposed a logistic equation with two different delays to mimic the population $x(t)$ of the Australian blowfly *Lucila cuprina*, which is represented as follows:

$$\frac{dx}{dt} = rx(t)\left[1 + ax(t-\tau_1) - bx(t-\tau_2)\right], \tag{D.8}$$

where $r > 0$, $a > 0$ and $b > 0$ are real constants, $\tau_1 > 0$ and $\tau_2 > 0$ corresponds to regeneration and reproductive delays, respectively.

### *D.3.2 Wilson and Cowan Model*

Wilson and Cowan [9, 10] model describes the evolution of a network of synaptically interacting neural populations, typically one being excitatory and the other inhibitory, in the presence of two different delays represented as

$$\frac{dx}{dt} = -x(t) + f\left[\theta_x + ax(t-\tau_1) + by(t-\tau_2)\right], \tag{D.9}$$

$$\frac{dy}{dt} = \alpha\left(-y(t) + f\left[\theta_y + cx(t-\tau_2) + dy(t-\tau_1)\right]\right), \tag{D.10}$$

where $x(t)$ and $y(t)$ represent the synaptic activity of the two populations with a relative time scale for the response set by $\alpha^{-1}$. The architecture of the network is fixed by the weights $a, b, c, d$, while $\theta_{x,y}$ describe background drives and $f$ is the common firing rate function.

### *D.3.3 Human Respiratory Model*

A simple model of the respiratory control mechanism in humans is represented as [11]

$$\frac{dx}{dt} = p - \alpha W\left[x(t-\tau_1), y(t-\tau_2)\right](x(t) - x_I), \tag{D.11}$$

$$\frac{dy}{dt} = -\sigma + \beta W\left[x(t-\tau_1), y(t-\tau_2)\right](y(t) - y_I), \tag{D.12}$$

where $x(t)$ and $y(t)$ denote the arterial $CO_2$ and $O_2$ concentrations, respectively. $W(\cdot,\cdot)$ is the ventilation function (the volume of gas moved by the respiratory systems), $\tau_{1,2}$ are transport delays, $x_I$ and $y_I$ are inspired $CO_2$ and $O_2$ concentrations, $p$ is the $CO_2$ production rate, $\sigma$ is the $O_2$ consumption and $\alpha$, $\beta$ are positive constants referring to the diffusibility of $CO_2$ and $O_2$, respectively.

## D.4 DDEs with Distributed Delay

In the following we will present a few examples for DDEs with distributed delay in addition to the details presented in Sect. 1.1.3.

### *D.4.1 Volterra's Logistic Equation*

The Hutchinson's equation (D.1) assumed that the regulatory effect depends on the population at a fixed earlier time $t - \tau$. However, in a more realistic model the delay effect should be an average over past populations and this requires an equation with a distributed delay. Volterra [2, 12] suggested the first model of logistic equation with distributed delay and he used a distributed delay term to examine a cumulative effect in the death rate of a species, depending on the population at all times, represented as

$$\frac{dx}{dt} = rx(t)\left[1 + \frac{1}{K}\int_{-\infty}^{t} G(t-s)x(s)ds\right], \tag{D.13}$$

where $G(t)$ is the delay kernel, corresponding to a weighting factor which indicates how much emphasis should be given to the size of the population at earlier times to determine the present effect on resource availability.

### *D.4.2 Neural Network with Distributed Delay*

Hopfield neural networks with distributed delays are considered [13] to take into account the distribution of conduction velocities along parallel pathways with a variety of axon sizes and lengths as [13]

$$\frac{dx}{dt} = -x(t) + a\tanh\left[x(t) - b\int_{0}^{\infty} x(t-s)k(s)ds - c\right], \tag{D.14}$$

where $x(t)$ is the state of neuron, $a$, $b$ and $c$ are non-negative constants.

### D.4.3 Chemostat Model

A chemostat model of a single species feeding on a limiting nutrient supplied at constant rate is proposed as [14]

$$\frac{dS}{dt} = \left(S^0 - S(t)\right) D - ax(t)p\left(S(t)\right), \tag{D.15}$$

$$\frac{dx}{dt} = x(t)\left[-D_1 + \int_{-\infty}^{t} F(t-s)p(S(t))ds\right], \tag{D.16}$$

where $S(t)$ and $x(t)$ denote the concentration of the nutrient and the population of microorganism at $t$. $S^0$ denotes the input concentration of nutrient, $D$ is referred to as the dilution rate and $D_1$ denotes the sum of the dilution rate and the death rate of the population of microorganism. The function $p(S)$ describes the species specific growth rate and $a^{-1}$ is referred to as the growth yield constant.

## D.5 DDEs with State-Dependent Delay

We will discuss some of the DDEs with state-dependent delay that have been used in the literature in some detail. General discussion and some other examples are presented in Sect. 1.1.4,

### D.5.1 Population Model

Considering the birth rate as population density dependent rather than age dependent certain population dynamics is also modeled with delay equations with state dependent delay. Assuming the lifespan $L$ of individuals in the population as a function of the current population size, $x(t)$, and taking into account the crowding effect, a DDE with state dependent delay for population dynamics is suggested [15, 2],

$$\frac{dx}{dt} = \frac{bx(t) - bx(t - L\left[x(t)\right])}{1 - L'\left[x(t)\right]bx(t - L\left[x(t)\right])}. \tag{D.17}$$

### D.5.2 Logistic Model with State Dependent Delay

Logistic model with a state dependent delay has also been proposed [2],

$$\frac{dx}{dt} = rx(t)\left[1 - \frac{x(t - \tau(x(t)))}{K}\right]. \tag{D.18}$$

### *D.5.3 Mechanical Model for Machine Tool Chatter*

Turning process in machine tool chatter is governed by the following state dependent DDE [16],

$$m\ddot{x}(t) + c_x\dot{x}(t) + k_x x(t) = K_x w\left[v\tau(x_t) + y(t - \tau(x_t)) - y(t)\right]^q, \quad \text{(D.19)}$$

$$m\ddot{y}(t) + c_y\dot{y}(t) + k_y y(t) = K_y w\left[v\tau(x_t) + y(t - \tau(x_t)) - y(t)\right]^q, \quad \text{(D.20)}$$

where $m$, $c_x$, $c_y$, $k_x$ and $k_y$ are the modal mass, the damping and the stiffness parameters in the $x$ and $y$ directions, respectively. $K_{x,y}$ are the cutting coefficients, $w$ is the depth of cut, $q$ is an exponent and $v$ is the speed of feed. More details on the system and its stability analysis can be found in [16].

## D.6 DDEs with Time-Dependent Delay

In the following we will present explicit equations for two models described by DDEs with time-dependent delays.

### *D.6.1 Stem-Cell Equation*

The stem cell equation can be put in the form [17]

$$\dot{S}(t) = 2M(t - \tau_m(t))S(t - \tau_m(t)) - S(t)\left[M(t) + \omega\right], \quad \text{(D.21)}$$

where $S(t)$ is the available stem cell population. The rate $M(t)S(t)$ at which stem cells enter the mitotic channel is controlled by the mitotic operator, $M(t)$, acting on the stem cell population and the rate at which they return after dividing is $2M(t - \tau_m(t))S(t - \tau_m(t))$, assuming that there are no losses. $\tau_m(t)$ represents the delay between cells leaving the stem cell population to enter the mitotic cycle and the return of two daughter cells.

### *D.6.2 Neural Network Model*

A neural network model with time-varying delay is represented as [18]

$$\frac{dX}{dt} = -DX(t) + AG(X(t)) + BF(X(t - \tau(t))) + I(t), \quad \text{(D.22)}$$

where $X(t) = [x_1(t), x_2(t), \cdots, x_n(t)]$ is the state vector of the network at time $t$, $D = \text{diag}\,[d_1, d_2, \cdots, d_n]$ with $d_i > 0$ denotes the rate with which the cell $i$ resets its potential to the resting state when isolated from other cells and inputs,

$A = (a_{kl})_{n\times n}$, $B = (b_{kl})_{n\times n} \in \mathbb{R}^{n\times n}$ represent the connection weight matrix and the delayed connection weight matrix, respectively. $a_{kl}, b_{kl}$ denote the strengths of connectivity between the cell $k$ and $l$ at time $t$ and $t - \tau(t)$, respectively. $F(X) = \big[f_1(x_1(t)), \cdots, f_n(x_n(t))\big]$, $G(X) = \big[g_1(x_1(t)), \cdots, g_n(x_n(t))\big]$ are activation functions.

Further details on all these examples can be found in their respective references.

## References


1. G.E. Hutchinson, Ann. N.Y. Acad. Sci. **50**, 221 (1948)
2. S. Ruan, Delay differential equations in single species dynamics, in *Delay Differential Equations and Applications*, ed. by O. Arino et al. (Springer, Berlin, 2006), pp. 477–517
3. K. Gopalsamy, G. Ladas, Quart. Appl. Math. **48**, 433 (1990)
4. M.C. Mackey, Blood **51**, 941 (1978)
5. M.C. Mackey, Dynamic haematological disorders of stem cell origin, in *Biophysical and Biochemical Information Transfer in Recognition*, ed. by J.G. Vassileva-Popova, E.V. Jensen (Plenum Press, New York, 1979), pp. 373–409
6. J.G. Milton, A. Longtin, Vision Res. **30**, 515 (1990)
7. J.G. Milton, A. Longtin, T.H. Krikham, G.S. Francis, Am. J. Ophthalmol. **105**, 402 (1988)
8. R.D. Braddock, P. van den Driessche, J. Austral. Math. Soc. Ser. B **24**, 292 (1983)
9. H.R. Wilson, J.D. Cowan, Biophys. J. **12**, 1 (1972)
10. S. Coombes, C. Laing, Philos. Trans. R. Soc. A **367**, 1117 (2009)
11. K.L. Cooke, J. Turi, J. Math. Biol. **32**, 535 (1994)
12. V. Volterra, C.R. Acad. Sci. **199**, 1684 (1934)
13. F.Y. Zhang, H.F. Huo, Discrete Dyn. Nat. Soc. **2006**, 27941 (2006)
14. S. Ruan, G.S.K. Wolkowicz, J. Math. Anal. Appl. **204**, 786 (1996)
15. J. Bélair, Population models with state-dependent delay, in *Mathematical Populations Dynamics*, ed. by O. Arino, D.E. Axelrod, M. Kimmel (Marcel Dekker, New York, 1991), pp. 165–176.
16. T. Insperger, D.A.W. Barton, G. Stépán, Int. J. Non-linear Mech. **43**, 140 (2008)
17. J. Kirk, T.E. Wheldon, W.M. Gray, J.S. Orr, Bio-Med. Comput. **1**, 291(1970)
18. W. Wang, J. Cao, Physica A **366**, 197 (2006)

# Glossary

**Amplitude death** The phenomenon of suppression of oscillations in dynamical systems mainly due to time-delay feedback or time-delay coupling is termed as amplitude death.

**Analog simulation circuit** An electronic circuit designed to mimic the dynamics of a system modelled by a linear/nonlinear evolution equation.

**Analytic signal approach** It is one of the approaches to calculate the phase of a non-phase-coherent chaotic/hyperchaotic attractor. The complex analytical signal $\chi(t)$ is constructed from a scalar time series $s(t)$ via Hilbert transform (HT).

**Anticipatory synchronization** Anticipatory synchronization is a special kind of generalized synchronization (see below), where one (receiver) of the coupled systems anticipates the state of the other (transmitter) with finite anticipating time.

**Attractor** It is a bounded region of phase space of a dynamical system towards which nearby trajectories asymptotically approach. The attractor may be a point or a closed curve or an unclosed but bounded orbit.

**Autonomous system** A system with no explicit time-dependent term in its equation of motion.

**Band merging bifurcation** Merging of two or more bands of a $m$-band chaotic attractor at a critical value of a control parameter.

**Bifurcation** A sudden/abrupt qualitative change in the dynamics of a system at a critical value of a control parameter when it is varied smoothly.

**Bifurcation diagram** A plot illustrating qualitative changes in the dynamical behavior of a system as a function of a control parameter.

**Bifurcation route** The nature of sudden/abrupt qualitative changes in the dynamical behavior of a system as a function of a control parameter indicating the mechanism responsible for the change.

**Chaos** A phenomenon or process of occurrence of bounded nonperiodic evolution in deterministic nonlinear systems with high sensitive dependence on initial conditions. A consequence is that nearby chaotic orbits diverge exponentially (in a

time average sense) in phase space. A measure of quantification of the degree of divergence is the set of Lyapunov exponents. Chaotic motion is characterized by at least one positive Lyapunov exponent.

**Chimera state** The coexistence of coherent (synchronized) and incoherent (desynchronized) states in coupled identical oscillators is called a chimera state.

**Chua's circuit** A simple, third-order, autonomous electronic circuit consisting of two linear capacitors, a linear inductor, a linear resistor, and only one nonlinear element, namely Chua's diode, having a piecewise linear characteristic.

**Chemostat model** A chemostat (from *Chem*ical environment is *stat*ic) is a bioreactor to which fresh medium is continuously added, while culture liquid is continuously removed to keep the culture volume constant. By changing the rate with which the medium is added to the bioreactor the growth rate of the microorganism can be easily controlled.

**Complete synchronization** Complete synchronization (CS) refers to the identical evolution of the trajectories of two identical linear/nonlinear systems which is achieved by means of a suitable coupling in such a way that the two trajectories remain in step with each other in the course of time.

**Complex network** In the context of network theory, a complex network is a network (graph) with non-trivial topological features (Examples: scale-free networks and small-world networks) that do not occur in simple networks such as lattices or random graphs. The study of complex networks is an active area of scientific research of this decade inspired largely by the empirical study of real-world networks such as computer networks and social networks.

**Connection delay** Delay caused due to the finite time required for the propagation of signals from output to the receiver end or among the interconnected dynamical systems.

**Correlation dimension** A quantitative measure used to describe geometric and probabilistic features of attractors. It is an integer for regular attractors such as a fixed point, a limit cycle or a quasiperiodic orbit. It is non-integer for a strange (chaotic) attractor.

**Correlation function** A statistical measure used to characterize regular and chaotic motions. For periodic motion it oscillates while for chaotic motion it decays to zero.

**Correlation of probability of recurrence (CPR)** A cross correlation coefficient between the generalized autocorrelation functions of two systems, $P_{1,2}(t)$, is defined as correlation of probability of recurrence (CPR).

**Cross recurrence plot (CRP)** A cross recurrence plot (CRP) is a bivariate extension of the recurrence plot and was introduced to analyse the difference between two different systems. CRP can be regarded as a generalisation of the linear cross-correlation function.

**Delay differential equation (DDE)** A delay-differential equation (DDE) comprises of an unknown function and certain of its derivatives, evaluated at arguments that differ by fixed numerical values. For example, $\dot{x}(t) = F(t, x(t), x(t-\tau))$ is a retarded DDE for $\tau > 0$. DDEs (also called functional differential equations or retarded differential-difference equations) generalize the concept of differential equations by allowing the state of the system to depend on states different from the present one. DDEs can also be of neutral and advanced types.

**Delay time modulation (DTM)** Delay time modulation refers to the case of time varying delay $\tau(t)$, where the time-delay $\tau$ evolve in time or even it can be a function of state variable $\tau(x)$ (in which case it is referred to as state dependent delay).

**El Niño-Southern oscillation** The El Niño-Southern Oscillation is often abbreviated as ENSO and in popular usage is called simply El Niño. It is defined by sustained differences in the Pacific ocean surface temperatures when compared with the average value. The accepted definition is a warming or cooling of at least 0.5 °C(0.9 °F) averaged over the east-central tropical Pacific ocean. When this happens for less than 5 months, it is classified as El Niño or La Niña conditions; if the anomaly persists for 5 months or longer, it is called an El Niño or La Niña "episode". Typically, this happens at irregular intervals of 27 years and lasts 9 months to 2 years.

**Embedding theorem** Delay embedding theorem gives the conditions under which a chaotic dynamical system can be reconstructed from a sequence of observations of the state of a dynamical system. The reconstruction preserves the properties of the dynamical system that do not change under smooth coordinate changes, but it does not preserve the geometric shape of structures in phase space.

**Epidemiology** It is a branch of science dealing with spreading of diseases in human population. The model proposed to study the nature of spreading and to identify the measures to control a specific disease is called an epidemic model. The term "epidemics" is derived from Greek *epi-* upon + *demos* people. An epizootic is the analogous circumstance within an animal population.

**Equilibrium point** An admissible solution of $F(X) = 0$ for a dynamical system $\dot{X} = F(X)$, $X = (x_1, x_2, \cdots, x_n)^T$. It is also called fixed point or singular point of the system.

**Error feedback** Error feedback refers to the feedback given as a linear/nonlinear function of the difference of the state variables of the coupled systems.

**Feedback delay** Finite time taken by a signal that is fed back into the system causes the feedback delay. For instance, in semiconductor lasers the coherent light is converted into chaotic signal due to the feedback of the light through a cavity and the round trip time results in the feedback delay. Feedback delay can give rise to plethora of new behaviors in dynamical systems (see Chaps. 5 and 6).

**FitzHugh-Nagumo oscillator** FitzHugh-Nagumo model $\dot{x} = x - x^3/3 - y + I$, $\dot{y} = 0.08(x + 0.7 - 0.8y)$ is a two-dimensional simplification of the Hodgkin-Huxley

model of spike generation in squid giant axons. It is used to isolate conceptually the essentially mathematical properties of excitation and propagation from the electrochemical properties of sodium and potassium ion flow.

**Generalized autocorrelation function** In recurrence quantification analysis, generalized autocorrelation function, $P(\varepsilon, t)$, can be considered as the probability that the system recurs to the $\varepsilon$-neighbourhood of a former point $\mathbf{x}_i$ of the trajectory after $t$ time steps. Comparing $P(\varepsilon, t)$ of two systems, one can characterize quantitatively and qualitatively the existence of phase synchronization between the two systems.

**Generalized synchronization** Synchronization can be achieved even in the case of coupled non-identical systems and in this case, it is termed as generalized synchronization where there exists some functional relationship between the variables of the coupled systems.

**Globally coupled chimera (GCC) state** The coexistence of chimera states in a system of identical oscillators with (sub) populations with time-delay coupling is termed as globally coupled chimera states. It is demonstrated that coupling delay can induce globally clustered chimera (GCC) states in systems having more than one coupled identical oscillator (sub) populations. By GCC one refers to the state of a system, which has more than one (sub) population, that splits into two different groups, one synchronized and the other desynchronized, each group comprising of oscillators from both the populations.

**Hopf bifurcation** It corresponds to the birth of a limit cycle from an equilibrium point when a control parameter is varied. If the limit cycle is stable (unstable) then the bifurcation is called supercritical (subcritical).

**Hyperchaos** It represents chaotic motion with more than one positive Lyapunov exponents. It has at least two exponentially diverging directions in its orthonormal phase space.

**Ikeda system** Ikeda system was introduced to describe the dynamics of an optical bistable resonator, which is specified by the state equation $\frac{dx}{dt} = -\alpha x(t) - \beta \sin x(t - \tau)$. Physically $x(t)$ is the phase lag of the electric field across the resonator and thus may clearly assume both positive and negative values, $\alpha$ is the relaxation coefficient, $\beta$ is the laser intensity injected into the system and $\tau$ is the round-trip time of the light in the resonator.

**Intermittency route to chaos** A route to chaos where regular orbital behavior is intermittently interrupted by short time irregular bursts. As the control parameter is varied, the durations of the bursts increase, leading to full scale chaos.

**Inverse period doubling** It denotes the bifurcation sequence of a nonlinear dynamical system which is inverse to the period doubling bifurcation as a control parameter is varied.

**Invertible map** A map is invertible when its inverse exists and is unique for each point in the phase space.

**Jacobian matrix** Jacobian matrix is the matrix of all first-order partial derivatives of a vector-valued function. The Jacobian determinant (often simply called the Jacobian) is the determinant of the Jacobian matrix. These concepts are named after the mathematician Carl Gustav Jacob Jacobi.

**Joint recurrence plot (JRP)** A joint recurrence plot is introduced to compare the states of different systems by estimating the recurrences of their trajectories in their corresponding phase spaces separately and then look for the times when both of them recur simultaneously, that is when joint recurrence occurs.

**Kelvin waves** A Kelvin wave is a wave in the ocean or atmosphere that balances the earth's Coriolis force against a topographic boundary such as a coastline, or a waveguide such as the equator. A feature of a Kelvin wave is that it is non-dispersive, i.e., the phase speed of the wave crests is equal to the group speed of the wave energy for all frequencies. This means that it retains its shape in the alongshore direction over time.

**Krasovskii-Lyapunov theory** Krasovskii-Lyapunov theory is the direct extension of Lyapunov second theorem on stability, which states that if a positive definite function $V(x) : R^n \rightarrow R$ exists such that $V(x) \geq 0$ with equality if and only if $x = 0$ and $\dot{V}(x) \leq 0$ with equality if and only if $x = 0$ (negative definite), then the equilibrium state is Lyapunov stable.

**Kuramoto oscillators** It is a mathematical model used to describe synchronization. More specifically, it is a model for the behavior of a large set of coupled oscillators. Its formulation was motivated by the behavior of systems of chemical and biological oscillators, and it has found widespread applications. The most popular form of the model has the following governing equations: $\frac{d\theta_i}{dt} = \omega_i + \frac{K}{N}\sum_{j=1}^{N}\sin(\theta_j - \theta_i)$, $i = 1 \ldots N$, where the system is composed of N limit-cycle oscillators.

**Lag synchronization** Lag synchronization is a special case of generalized synchronization, where one of the coupled systems always evolve in lag with respect to the other with a finite lag time.

**Limit cycle** An isolated closed orbit in the phase space associated with a dynamical system.

**Linear superposition principle** A property associated with linear differential equations. The property is that if $u_1$ and $u_2$ are two linearly independent solutions of a linear homogeneous differential equation then $u = au_1 + bu_2$ is also a solution of it, where $a$ and $b$ are arbitrary (complex) constants.

**Localized set** It refers to the sets obtained by observing one of the coupled systems whenever a defined event occurs in the other system and viceversa. The concept of localized sets has been introduced recently as a new framework to identify phase

synchronization in chaotic/hyperchaotic attractors without explicitly calculating the phase variable.

**Logistic map** A discrete map analog of the logistic equation for population growth. The map is represented as $x_{n+1} = ax_n(1 - x_n)$, where $a$ is a parameter with $0 \leq a \leq 4$ and $0 < x < 1$.

**Lorenz equation** The paradigmic nonlinear chaotic system originally introduced by E. Lorenz in 1963 in connection with atmospheric convection, represented by a set of three coupled ordinary differential equations $\frac{dx}{dt} = \sigma(y-x)$, $\frac{dy}{dt} = x(\rho-z)-y$, $\frac{dz}{dt} = xy - \beta z$, where $\sigma$ is called the Prandtl number and $\rho$ is called the Rayleigh number.

**Lyapunov exponent** Lyapunov exponent of a dynamical system is a quantity (a number) that characterizes the rate of separation of infinitesimally close trajectories. Different types of orbits can be distinguished depending on the value of its Lyapunov exponents. All negative exponents represent regular and periodic orbits, while at least one positive exponent indicates the presence of chaotic motion. More than one positive exponent indicate the presence of hyperchaotic motion.

**Lyapunov function** Lyapunov function is a function which can be used to prove the stability of a certain fixed point in a dynamical system or autonomous differential equation.

**Mackey-Glass system** The Mackey-Glass system, which was originally deduced as a model for blood production in patients with leukemia, can be represented by the first order nonlinear DDE $\dot{x} = -bx(t) + \frac{ax(t-\tau)}{(1.0+x(t-\tau)^c)}$, where $a$, $b$ and $c$ are positive constants. Here, $x(t)$ represents the concentration of blood at time $t$ (density of mature cells in bloodstreams), when it is produced, $x(t-\tau)$ is the concentration when the "request" for more blood is made and $\tau$ is the time-delay between the production of immature cells in the bone marrow and their maturation for release in circulating bloodstreams.

**Noise** In common use, the word noise means any unwanted sound. In both analog and digital electronics, noise is an unwanted perturbation to a wanted signal. In signal processing or computing it can be considered unwanted data without meaning.

**Nonautonomous system** A system with at least one explicit time-dependent term in its equation of motion.

**Non-invertible map** Maps that are not invertible are non-invertible maps, that is, one for which inverse does not exist.

**Non-phase-coherent attractor** If the flow of a dynamical system does not have a proper center of rotation around a fixed reference point, then the corresponding attractor is termed as a non-phase-coherent attractor. For instance, the funnel Rössler attractor for the parameter values $a = 0.25$, $b = 0.2$, and $c = 8.5$ shown in Fig. 10.1b of Chap. 10, is an example of non-phase-coherent attractor.

**Orthonormalization** A form of orthogonalization in which the resulting vectors are all unit vectors. Gram-Schmidt orthogonalization, also called the Gram-Schmidt process, is a procedure which takes a nonorthogonal set of linearly independent functions and constructs an orthogonal basis over an arbitrary interval with respect to an arbitrary weighting function $w(x)$.

**Phase-coherent attractor** If the flow of a dynamical system has a proper rotation around a fixed reference point as its center, then the corresponding attractor is called a phase-coherent attractor. For instance, Rössler attractor for the standard parameter values $a = 0.15, b = 0.2$, and $c = 8.5$ shown in Fig. 10.1a of Chap. 10, is an example of phase-coherent attractor.

**Period doubling** It denotes the bifurcation sequence of periodic motions for a nonlinear dynamical system in which the period doubles at each bifurcation as a control parameter is varied. Beyond a critical accumulation parameter value, chaotic motion occurs. It is also referred as subharmonic bifurcation or flip bifurcation.

**Phase flip bifurcation** It denotes the abrupt change in the relative phase of the coupled oscillators from zero to $\pi$ as a function of the delay time.

**Phase point** A point in the phase space representing the state of a system at any instant of time.

**Phase space** As abstract space where each of the variables needed to specify the dynamical state of a system represents an orthogonal coordinate.

**Phase synchronization** Phase synchronization can be defined as perfect locking of the phase/frequency of the coupled systems, while their amplitudes remain uncorrelated and often chaotic in the case of coupled chaotic systems.

**Piecewise linear system** A piecewise linear system is usually referred to a nonlinear dynamical system, whose nonlinear function $f(x)$ is composed of piecewise linear segments.

**Poincaŕe section** Any suitable hyperplane of the phase space is a Poincaŕe section (or surface of section). The relation between the successive intersections of the phase trajectories with this section in a single direction constitutes the Poincaŕe map.

**Propagation delay** See connection delay.

**Pseudospace** Any additional phase space created by embedding technique is referred to as pseudospace.

**PSPICE simulation** PSPICE, is an acronym for Personal Simulation Program with Integrated Circuit Emphasis, is a SPICE (Simulation Program with Integrated Circuit Emphasis) analog circuit and digital logic simulation software that runs on personal computers.

**Recurrence analysis** Recurrence analysis is a powerful technique that visualizes the recurrences of a dynamical system and gives information about the behavior of its trajectory in the phase space.

**Recurrence plot (RP)** A recurrence plot (RP) is the graphical representation of a binary symmetric square matrix which encodes the times when two states are in close proximity (neighbours), that is the time of recurrence in the phase space.

**Recurrence quantification analysis (RQA)** Several measures of complexity which quantify the small scale structures in recurrence plots have been proposed and are known as recurrence quantification analysis (RQA).

**Rossby waves** Rossby waves are giant meanders in high-altitude winds that are a major influence on weather. Their emergence is due to shear in rotating fluids so that the Coriolis force changes along the sheared coordinate. In planetary atmospheres, they are due to the variation in the Coriolis effect with latitude. The waves were first identified in the Earth's atmosphere in 1939 by Carl-Gustaf Arvid Rossby who went on to explain their motion. Rossby waves are a subset of inertial waves.

**Rössler system** Otto Rössler designed the Rössler attractor in 1976, but the theoretical equations were later found to be useful in modeling equilibrium in chemical reactions. The defining equations are: $\frac{dx}{dt} = -y-z$, $\frac{dy}{dt} = x+ay$, $\frac{dz}{dt} = b+z(x-c)$. Rössler studied the chaotic attractor with $a = 0.2, b = 0.2$, and $c = 5.7$, though properties of $a = 0.1, b = 0.1$, and $c = 14$ have been more commonly used since.

**Runge-Kutta method** In numerical analysis, the Runge-Kutta methods are an important family of implicit and explicit iterative methods for the approximation of solutions of ordinary differential equations. These techniques were developed by the German mathematicians C. Runge and M.W. Kutta.

**Stochastic process** A stochastic process is the counterpart to a deterministic process (or deterministic system). Instead of dealing with only one possible "reality" of how the process might evolve under time (as is the case, for example, for solutions of an ordinary differential equation), in a stochastic or random process there is some indeterminacy in its future evolution described by probability distributions. This means that even if the initial condition (or starting point) is known, there are many possibilities the process might go to, but some paths are more probable and others less.

**Synchronization** The word *synchronous* is derived from Greek terminology *chronous* means time and *syn* means common. Put together synchronous/synchronization has its direct meaning "share the common time" or "occurring in the common time". Technically, it can be defined as "entrainment of a dynamical property/share a common property of motion" or "as degree of correlation" between the interacting dynamical systems.

**Time series** The measured values of a physical variable of a dynamical system at regular intervals of time.

**Transient motion** An initial time evolution of a system before getting settled into its steady state behavior.

**Unstable periodic orbit** An unstable period-1, or $2, \cdots$, or $n$ fixed point or limit cycle. A chaotic orbit is regarded as a pool of unstable periodic orbits.

# Index